Solar Energy 207 (2020) 110–132

Contents lists available at ScienceDirect

Solar Energy

journal homepage: www.elsevier.com/locate/solener

Review of heliostat calibration and tracking control methods

Johannes Christoph Sattler[a], Marc Röger[b,*], Peter Schwarzbözl[c], Reiner Buck[d], Ansgar Macke[e], Christian Raeder[f], Joachim Göttsche[a]

[a] Solar-Institut Jülich (SIJ) of the Aachen University of Applied Sciences, Heinrich-Mussmann-Str. 5, 52428 Juelich, Germany
[b] German Aerospace Center (DLR), Institute of Solar Research, Paseo de Almería 73, 04001 Almería, Spain
[c] German Aerospace Center (DLR), Institute of Solar Research, Linder Hoehe, 51147 Cologne, Germany
[d] German Aerospace Center (DLR), Institute of Solar Research, Pfaffenwaldring 38-40, 70569 Stuttgart, Germany
[e] CSP Services GmbH, Friedrich-Ebert-Ufer 30, 51143 Cologne, Germany
[f] German Aerospace Center (DLR), Institute of Solar Research, Karl-Heinz-Beckurts-Str. 13, 52428 Juelich, Germany

ARTICLE INFO

Keywords:
Heliostat
Control
Calibration
Alignment
Central receiver system
Solar power tower

ABSTRACT

Large scale central receiver systems typically deploy between thousands to more than a hundred thousand heliostats. During solar operation, each heliostat is aligned individually in such a way that the overall surface normal bisects the angle between the sun's position and the aim point coordinate on the receiver. Due to various tracking error sources, achieving accurate alignment ≤1 mrad for all the heliostats with respect to the aim points on the receiver without a calibration system can be regarded as unrealistic. Therefore, a calibration system is necessary not only to improve the aiming accuracy for achieving desired flux distributions but also to reduce or eliminate spillage. An overview of current larger-scale central receiver systems (CRS), tracking error sources and the basic requirements of an ideal calibration system is presented. Leading up to the main topic, a description of general and specific terms on the topics heliostat calibration and tracking control clarifies the terminology used in this work. Various figures illustrate the signal flows along various typical components as well as the corresponding monitoring or measuring devices that indicate or measure along the signal (or effect) chain. The numerous calibration systems are described in detail and classified in groups. Two tables allow the juxtaposition of the calibration methods for a better comparison. In an assessment, the advantages and disadvantages of individual calibration methods are presented.

1. Introduction

In the past decade, the central receiver system (CRS) technology (also referred to as solar power tower plant, power tower or solar tower) has been subject to major technological advances which include not only the further development of individual system components but also the clear move towards constructing plants with high electrical power outputs. A good overview is given in a database created by SolarPACES (NREL, 2020). Currently, there are 10 plants of significant electrical output in operation (≥50 MW_e). These are Ivanpah (377 MW_e, USA, 2014), Khi Solar One (50 MW_e, South Africa, 2016), Huanghe Qinghai Delingha (135 MW_e, China, 2017), SUPCON Solar Delingha (50 MW_e, China, 2018), Shouhang Dunhuang 100 MW Phase II (100 MW_e, China, 2018), Noor Ouarzazate III (150 MW_e, Morocco, 2018), Power China Gonghe (50 MW_e,China, 2019), Luneng Haixi (50 MW_e, China, 2019), Ashalim Plot B (121 MW_e, Israel, 2019) and Hami (50MW_e, China, 2019). Today's large-scale CRS plants have large solar fields with tens of thousands of heliostats whereby the furthest distances of a heliostat from the tower are currently in the range between 1 and 1.77 km. Heliostats exist in all sorts of sizes. Examples are 1.14 m^2, 2 m^2, 8 m^2 or 15 m^2 (small mirror area), 48.5 m^2 (medium mirror area) and 96 m^2, 115.7 m^2, 140 m^2 and 178.5 m^2 (large mirror area). Usually a heliostat is designed with multiple mirror facets. Each heliostat individually tracks the angle bisector between sun and receiver by means of two computer-controlled drives. The tolerance for the heliostat accuracy, the so-called tracking error (i.e. the deviation of the heliostat actual orientation from the desired orientation) is extremely small, as illustrated by the following example: for a heliostat at a distance of 1 km north from the tower a tracking error of 1 mrad (equivalent to a 0.057°) results in an offset of around 2 m between the heliostat's desired aim point and the actual position of the solar focus on the receiver plane. The tolerance of the misalignment of a heliostat depends on the requirements defined by the plant developer, which is individual for each CRS system.

* Corresponding author.
E-mail address: marc.roeger@dlr.de (M. Röger).

https://doi.org/10.1016/j.solener.2020.06.030
Received 7 February 2020; Received in revised form 18 May 2020; Accepted 6 June 2020
Available online 30 June 2020

Nomenclature

C	component
CRS	central receiver system
CCD	charge-coupled device
CPU	central processing unit
E	estimated value by authors
FFT	fast Fourier transform
G	Group of heliostats that can be calibrated simultaneously (max. number of heliostats in a group depends on capability of calibration system)
GCS	global coordinate system
LCOE	levelised cost of electricity
LED	light-emitting diode
M	monitoring or measuring devices
MEMs	microelectromechanical systems
min	minute(s)
OCS	online calibration system
P	parallel calibration process (simultaneous calibration of all heliostats)
PSA	Plataforma Solar de Almería
RC	Regular calibration
R-CNN	region convolutional neural network
s	second(s)
S	sequential calibration process (calibration of one heliostat after another)
UAV	unmanned aerial vehicle

Greek letters

σ	Standard deviation from the mean

Subscript

e	electric

A tracking error can occur due to several reasons and there are various publications that describe error sources. As errors accumulate, they can lead to heliostat image drift, which is a deviation from ideal tracking whereby the image displaces away from the intended aim point over the course of time as described by Mancini (1999). In an extensive study by Jones and Stone (1999a), the heliostat tracking error sources at the Solar Two plant were scrutinised and described in detail. More recently, Díaz-Félix et al. (2013) evaluated heliostat field global tracking error distributions. Some of the errors named in the latter two publications include gravity bending, pivot point offset, atmospheric refraction, angular offset in the reference position of the tracking mechanisms, imperfect levelling of the heliostat pedestal and lack of perpendicularity between the tracking axes amongst other errors. Gross and Balz (2019) point out that tracking errors are also caused by disagreements between coordinate systems used by solar, civil and surveying engineers e.g. during the surveying process of a CSP site and due to programming errors. A detailed, comprehensive study carried out by Freeman et al. (2014), whose focus was to study the errors that affect the design of calibration and control systems, evaluated the impacts of individual errors. According to this study, errors with strong impact are due to *sensor and actuator errors* (gear ratio choice, backdrive of the heliostat, low encoder resolution) as well as *installation errors* (pedestal tilt, azimuth and elevation reference angle, non-level terrain). Further errors from the aforementioned categories but with medium impact are also listed and include dimensional tolerances in the drive wheel and gear backlash. The category *heliostat mirror errors* contains errors with medium impact such as deformation due to wind loading. The study further offers potential solutions to reduce the effects of the identified errors. From the above three studies it becomes evident that heliostat tracking errors are common and that it is most unlikely that heliostats can be designed and installed at a reasonable cost without at least a few errors with stronger impact. When considering the global tracking error (i.e. sum of individual heliostat errors) and the previously mentioned marginal tracking tolerances, it becomes clear that spillage and inaccurate heliostat orientation are two major issues for CRS plants. A heliostat tracking accuracy of ≤ 1 mrad should generally be aimed for. According to Jones and Stone (1999b) the energy collected by the receiver of the Solar Two plant was in the range of 10 to 20% lower than anticipated. In an evaluation, it was suspected that the heliostat performance was reduced due to the tracking error. The suspicion was confirmed by observations of occasionally misaligned heliostats and excessive heat flux on the heat shield directly above and below the receiver.

In order to measure tracking errors, it is common and necessary practice to use a heliostat field **calibration system.** In publications, a heliostat calibration system is also referred to as an **alignment control system**, heliostat **tracking control method**, **track alignment method** or similar. For ease of reading, the terms **calibration system** or **calibration method** are used throughout this text. As presented in Section 2.2, there are various types of calibration systems which serve different

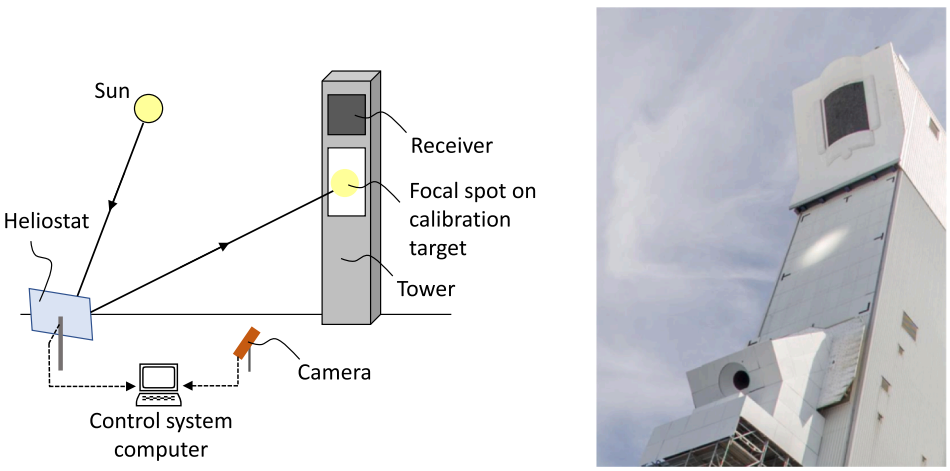

Fig. 1. Illustration of the camera-target method by Stone (1986) (left), Example of a Lambertian target with a solar focus during a calibration procedure at the Solar Tower Jülich, Germany (right). (Photo: DLR, CC-BY 3.0)

purposes. An ideal calibration system for larger-scale CRS (≥ 50 MW_e) should fulfil the following basic requirements: measurement of the heliostat alignment at high accuracy and precision in the range of 0.1 to 0.3 mrad whereby the entire heliostat field is repeatedly calibrated every few dozens of seconds (i.e. closed-loop feedback tracking control) as well as cost effectiveness. For most proposed or existing calibration methods the rule applies that in order to safely guarantee a desired overall heliostat tracking accuracy, it is necessary to measure 5–10 times more accurate. Most calibration methods must therefore measure at an accuracy of 0.1–0.2 mrad such that together with other inaccuracies such as deformation and wind effects or non-continuous tracking, the global error sums up to around 1 mrad. The specifications for the calibration accuracy are very hard to meet. A highly accurate calibration system will lead to a reduction in spillage losses and allow complex aiming strategies as well as a better flux distribution on the receiver. This, in turn, will increase the efficiency and thus have a positive effect on the levelised cost of electricity (LCOE).

Since the 1980s, several heliostat calibration methods have been developed by researchers and industry. An overview on the development of model based open-loop tracking methods is given by Malan (2014). Although the high number of published calibration methods and unique concepts show that much work in this field is being done, it is still uncertain which ones might be successful. All calibration systems are principally competing with the *Automatic Heliostat Track Alignment Method* patented by Stone (1986), which is – still nowadays – the state-of-the-art calibration method deployed by most commercial CRS plants as can be observed on photographs (cf. Fig. 1). In this paper, this method is referred to as camera-target method. A calibration is done by sequentially moving individual heliostats out of the receiver focus onto a white Lambertian target screen underneath the receiver, capturing the solar focus on the target screen using a camera on the ground and, in a final step, using image processing software to detect the centroid solar focus position on the target and comparing it to a reference position. By comparison of the solar focus position with the desired reference position, an alignment error can be computed. The measured alignment error is usually stored in a database and can be used as sampling data for an error model.

The next chapter is dedicated to general and specific terms on the two topics heliostat calibration and tracking control. Different heliostat calibration methods are described and classified in the third chapter. An assessment which includes a discussion of advantages and disadvantages of individual calibration methods is presented in the final fourth chapter. In this work, the authors endeavoured to comprehensively cover the range of existing and proposed calibration methods for which published information is available. The authors refrain from speculation in order to comply with scientific standards and objectiveness. Estimations given by the authors are based on experience and represent an opinion.

2. Terms and definitions

In this chapter, the definitions of general and specific terms on the topics *heliostat calibration* and *tracking control* are given to clarify descriptions in the subsequent chapters. In order to establish clear general and specific terms for researchers and industry on a common basis, a guideline should be developed that is similar to the SolarPACES *Heliostat Performance Testing Guideline* (Röger et al., 2020).

2.1. Definition of general terms

See Table 1.

2.2. Definition of specific terms

This section describes the types of calibration processes, types of tracking control methods, closed-loop tracking control, open-loop tracking control and tracking motions.

2.2.1. Types of calibration processes

Differentiating in their purposes and abilities, three types of calibration processes are defined:

Pre-calibration (synonym: **coarse calibration**)

During the commissioning phase of a central receiver system, the drive mechanisms (actuators) and encoders as well as the kinematics of each heliostat together with the control system need to be calibrated initially in order to coarsely align a heliostat with a desired orientation. Once coarsely aligned, the heliostat can be assessed by a more precise calibration system. This so-called pre-calibration or coarse calibration is necessary after the assembly of a heliostat in order to compensate the numerous small manufacturing and assembly errors that, in sum, often

Table 1
A brief definition of general terms.

Term	Definition
Sun position	Pair of angles (solar altitude or zenith angle and solar azimuth angle) in the “global” coordinate system of the central receiver system (GCS) describing the position of the sun in the sky at given time and day, see (Duffie and Beckmann, 2006, p. 13). Definition of GCS, see Röger et al. (2020)
Heliostat orientation or alignment	Pair of angles (or vector) describing the orientation of the heliostat normal in the “global” coordinate system of the central receiver system (GCS). Definition of GCS, see Röger et al. (2020)
Heliostat or concentrator normal	Mirror area weighted mean of the normal vectors of all mirror elements
Desired orientation	Pre-calculated, ideal orientation of a heliostat
Solar focus	Solar irradiance reflected by a heliostat that impinges on the focal area on the receiver or target
True or actual orientation	Real orientation of a heliostat, approximated by measured orientation of the heliostat normal
Measured orientation	Measured orientation of the heliostat (this is the true orientation including measurement error)
Tracking error or deviation	Deviation of heliostat true orientation from desired orientation (defined as 1-D or 2-D-value, details see Röger et al. (2020))
(Tracking) correction values or correction angles or angular correction	Pair of angles representing the correction values of the heliostat orientation, that means the difference between measured heliostat orientation and orientation indicated in the heliostat control system
Calibration (general)	“Operation that, under specified conditions, in a first step, establishes a relation between the quantity values with measurement uncertainties provided by measurement standards and corresponding indications with associated measurement uncertainties and, in a second step, uses this information to establish a relation for obtaining a measurement result from an indication.”* Derived definition for the calibration of heliostats: Finding a relation between the desired orientation given to the heliostat control system and the true orientation (which can be deduced by the heliostat’s solar focus on the target for example) *General definition defined by the BIPM (Bureau International des Poids et Mesures) www.bipm.org
Calibration parameter	Parameter(s) describing the mathematical relation between the indicated orientation and the true (here: measured) orientation of a heliostat; calibration parameters are usually obtained by mathematical correlation of the results of a calibration process

lead to a significant misalignment from the desired orientation. The coarse calibration is carried out at least once for which a low accuracy of around 3–10 mrad is sufficient. The calibrated main axes' orientations are returned to the control system, which processes them and, if misaligned, computes new axes orientation parameters.

Regular calibration (synonym: **fine calibration**)

For a recurring identification of a heliostats' orientation, a highly accurate calibration method needs to be deployed during the regular heliostat field operation. The accuracy of a regular calibration is required to be in the approximate range of 0.1–0.3 mrad so that the global heliostat tracking error is acceptable. Regular calibration leads to acquiring a large set of calibration points covering a representative range of sun positions. The results of each calibration action are stored in a data base and are used to calculate the required heliostat orientation (e.g. by correlation). Depending on the deployed calibration method, the interval between the regular calibration of the main axes' orientations of each heliostat can be within a few seconds as long as several weeks, especially for large heliostat fields. To increase the tracking accuracy the interval should be as small as possible. If the calibration of each heliostat is carried out within (tens of) seconds (ideally within the time interval of the tracking motion of the tracking mechanism of the heliostat), then the calibration method can be referred to as ***online calibration system*** (OCS), i.e. it is capable to closed-loop tracking control.

Recurring calibrations of heliostat-mounted measurement device

If a measurement device (e.g. camera and/or sensors) is attached to a heliostat, it is necessary to calibrate it for its first time use during the heliostat construction or installation phase. Moreover, a recurring calibration from time to time is required. This is done by means of carrying out calibration measurements and deducing correction values for determining the orientation of the measuring device in the heliostat coordinate system. These correction values are then implemented into the control system.

2.2.2. *Types of tracking control methods*

Tracking control (or heliostat control) is the (automated) operation of setting certain indicators (e.g. motor angles or drive positions) such that a desired heliostat orientation is obtained that is necessary to reflect the sun onto the aim point on a target or receiver. The accuracy, signal frequency, and the location where the feedback signal is created, define the type of tracking control. Definitions and descriptions for tracking control methods are published in Malan (2014) and Swart (2017). The terms open-loop and closed-loop tracking control found in literature, however, can lead to confusion. The reason for this is that the boundary between one and the other mode is continuous. Fig. 2 and Fig. 3 visualise this relationship. As indicated in Fig. 2 (left) from top to bottom, the signal or effect (e.g. mirror surface normal, or solar focus) flows along various typical components (C). These components are, for example, the CPU in the control room (C1), the controller (C2), actuator (C3), encoder (C4), a camera or sensor on the concentrator (C5), the mirror surface normals (C6) and the concentrator normal (C7) to the solar focus on the receiver or target (C8). Between these signals or effects, there are factors which influence the quality of the effect. For example, the movement of a camera or sensor (C5) mounted on the concentrator is influenced by upstream parameters such as the quality of data transmission and the kinematics of the actuator and the heliostat axes. How well the solar focus hits the target is further influenced by the quality of alignment of the camera or sensor on the concentrator, or the quality how well a concentrator normal represents the mirror facets' normals as a whole. Fig. 2 (right) shows different monitoring or measuring devices (M) that

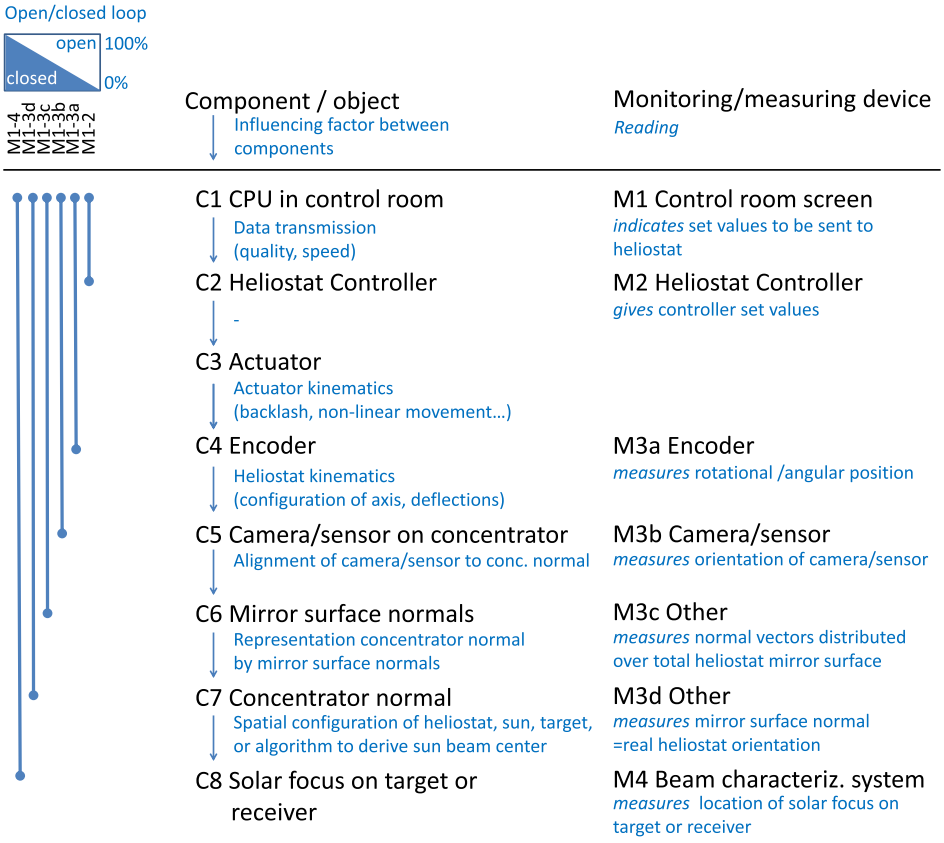

Fig. 2. Exemplary signal or effect chain from component C1 to C8 and the influencing factors between those (left) together with monitoring or measuring devices M1 to M4 and their readings (right).

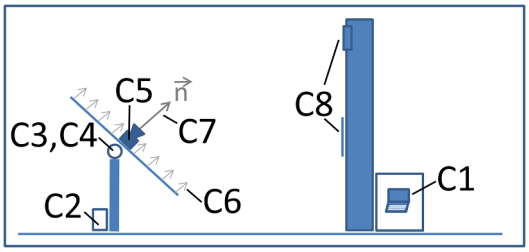

Fig. 3. Sketch of the components inside the signal/effect chain from control room CPU (C1) to the solar focus on the target (C8).

indicate or measure along the signal or effect chain. These include the control room screen (M1), the controller (M2), followed either by the encoder (M3a) or readings based on other measurement techniques (M3b, M3c, or M3d) or a beam characterisation system (M4). To elaborate on the above, alternatives of using a classical encoder (M3a) are, for example, the use of a camera or sensor(s) on the concentrator to measure the axes' orientations (M3b), a deflectometric approach (or by other means) that either measures the normal vectors of the mirror surfaces (M3c) or just the measurement of the heliostat normal vector (M3d). The measurement technique M3c requires further processing such that a single heliostat normal vector is calculated from the individual facets' normal vectors (M3c has the potential to be more accurate than M3d). Regarding (M4), the term beam characterisation system should be interpreted as solar focus characterisation system.

A fully closed-loop tracking control obtains its feedback from a technique that measures the area centres of the solar foci produced by each heliostat on the receiver (M4). A "partially" closed loop system, which measures the solar focus of each heliostat indirectly, receives its feedback from the monitoring devices (M3b, M3c or M3d). A more open-loop system receives feedback only from the encoders on the drive axis (M3a), although the internal control from M1 to M3a is technically considered as being closed-loop.

The authors strongly recommend that when discussing or writing about a closed-loop tracking control, it should be explicitly stated at which point in the signal chain the feedback signal is generated and hence which part of the whole chain is covered by the control loop (M1 through to M4 or less).

Closed-loop tracking control

In this paper, a minimum requirement for the control to be classified as a real or direct closed-loop tracking control is to receive feedback from M3b or higher with immediate, periodic response for all heliostats. The response must be sufficiently fast for step tracking, i.e. fast regarding the change in sun position and allowable tracking error (seconds). A closed-loop tracking control allows non-predictable, non-rigid heliostat kinematics. It should be noted though that if at the moment of a calibration perturbations occur due to wind, then the calibration and therefore also any tracking corrections may be erroneous. Moreover, gravity could also negatively influence the tracking control if its effect on the optical quality of the heliostat is not detected by the calibration system.

Open-loop tracking control

The heliostat is classified operating in open-loop tracking control mode if the tracking of the heliostat is solely based on feedback from the controller (M2, see Fig. 4a) or the encoder (M3a, see Fig. 4b) as well as the theoretical sun position and an initially and regularly determined set of calibration parameters (e.g. updated each week or month). This control mode can only be used for heliostats that are rugged and maintain significant properties such as rigidity, geometry, transmission ratio, etc. between two successive calibrations because no instant feedback of the result of the heliostat normal (M3d) or the solar focus on a target (M4) is returned. Here, the desired heliostat orientation is pre-calculated based on geometrical relations including a sun position algorithm. Heliostats using the state-of-the-art camera-target calibration method, as described in Stone (1986) for example, operate in open-loop tracking control.

Tracking motions

Two types of tracking motions can be distinguished: continuous tracking and step tracking. Although the sun's movement is continuous, stepwise tracking is the most commonly applied method. Here, the heliostat orientation is kept stationary while the reflected beam drifts towards or away from the desired aim point until the accumulated angular error surpasses a specified threshold. The heliostat orientation is corrected by a step movement of the drives. The statistical average tracking error related to this stepwise track correction can be in the range of 1 mrad, as pointed out by Kribus et al. (2004). They investigated the option of continuous tracking by using electronic speed controllers that allowed a smooth heliostat motion and were able to eliminate the error related to step tracking. Kribus et al. (2004) also suggested that real closed-loop tracking control should use continuous tracking to avoid perturbations through the step motion of the reflected beam.

3. Overview of heliostat calibration methods

An evaluation of published, patented and some new calibration systems are presented in this chapter. This includes characterising the calibration methods, sorting the methods into classes and describing them in more detail.

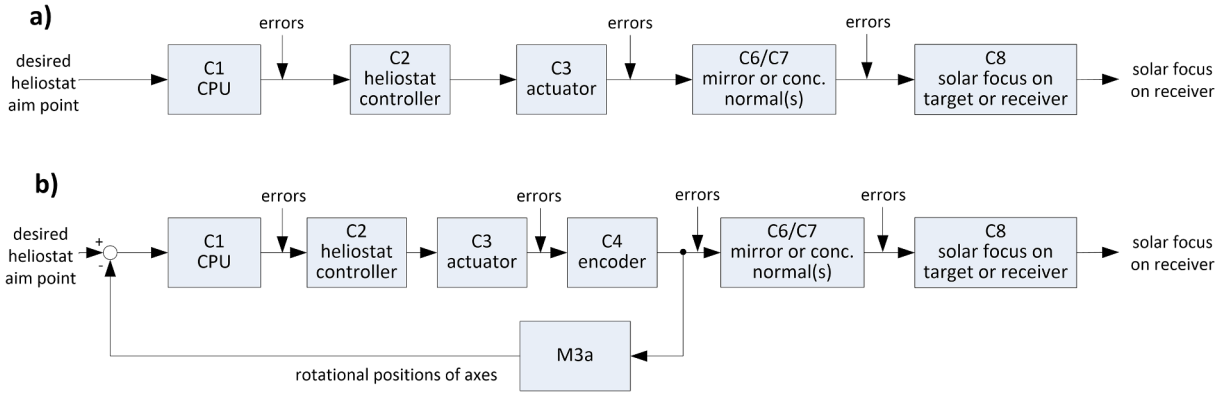

Fig. 4. Tracking control methods with a) pure feedforward control (open loop), and b) with encoder feedback (closed loop from M3a; overall classified also as open loop heliostat control, see description).

3.1. Classification of calibration methods

Malan (2014) describes in a generic control system diagram the control signal flows of calibration methods based on the *type of measurement signal information*, as illustrated in Fig. 5 below.

There are various possibilities to derive classification criteria. Including the above, altogether five groups of distinguished classification criteria were identified and resulting classes defined (see Table 2). In this paper a classification of calibration systems according to the criteria *Location, type and number of measuring devices or sensors* is chosen and used for all described calibration systems. Röger et al. (2018) presented a visualisation of this type classification, which is shown as a modified version in Fig. 6 and results in four classes labelled *class A* to *class D*. The classification depends on the location of the main device that is required for the calibration method.

3.2. Description of calibration methods

In this section, details on selected calibration methods are given. The calibration methods are classified in their respective classes as defined in Section 3.2. Moreover, an estimation is given with respect to the type of tracking control that can be realised with the individual calibration methods. For further data on the described calibration methods, refer to Table 3.

3.2.1. Class A: Central Camera(s) or Sensor(s)

Subclass A1 Camera(s) on ground

Class A1a: Camera-target method using the sun

At a specific moment, a single heliostat image is directed to the centre of a target. The deviation from its desired aimpoint is measured by taking and processing an image of a digital camera. Repeating this procedure for different points in time, the heliostat kinematics can be calibrated. Examples for this state-of-the art technique are described in King and Arvizu (1981) and Berenguel et al. (2004). A method patented by Bezares del Cueto et al. (2017) allows two or more heliostats to be calibrated simultaneously using several cameras positioned on the ground in the heliostat field. The cameras are oriented towards the target(s) or receiver zone and carry out solar focus centre calculations based on various image data in the visible, ultraviolet, near infrared and/or thermal infrared spectrum.

The heliostat orientation can be calibrated in the global coordinate system with high accuracy in the range of 0.1 mrad (authors' estimation) without using any extra device on the individual heliostats. More details can be found in Table 3. The signal flow is shown in Fig. 7.

Class A1b: Camera-target method using a signal beam or beam excitation

Similarly to class A1a, the calibration techniques A1b also use a straight-forward camera-target setup with subsequent image processing. The distinguishing feature, however, is that the heliostats' own beams or a secondary beam originating from the heliostats have a signalisation (i.e. coding). This allows distinguishing between the different heliostat beams.

The signalisation can be created by excitation through movement of the heliostat itself using its drives as suggested by Bern et al. (2016). The signalisation allows the superposition (and subsequent separation in the image processing) of one or ideally a large number of solar foci on the receiver surface itself or on the target area as well as solar foci around the receiver to detect spillage from misaligned heliostats.

Another type of signalisation is to generate a secondary low-energetic light beam from the concentrator surface which is directed to a target outside the receiver region, see e.g. Flesch et al. (2012) and Gross (2016). By measuring the position of that signal light beam and knowing the offset between the concentrator's main beam and the secondary beam, the heliostat orientation can be derived. The offset needs to be determined once; if the geometry remains constant over time no further offset re-calibration is necessary. The secondary light beam can be generated by means of mounting a small auxiliary mirror to the heliostat structure. The auxiliary mirror can be distinguished through temporal shadowing, colouring or by its shape. The method described by Flesch et al. (2012) is patented by Belhomme et al. (2011). The described methods use a camera on the ground that acquires an image of the auxiliary mirror's solar focus on the target. Fig. 8 (left) shows the principle of the method; Fig. 8 (right) shows a field test carried out by Flesch et al. (2012). Gross (2016) patented several variations of the signalisation method.

The heliostat orientation can be calibrated with high accuracy in the range of 0.2 mrad (authors' estimation) thus allowing a fine calibration. The error is slightly higher compared to the camera-target method due to the more challenging data processing to identify the correct beam in case of excitation as well as the uncertainty of the alignment of the device in case of the secondary light beam. More details can be found in Table 3. The signal flow is shown in Fig. 7.

Subclass A2 Camera(s) on tower or UAV(s)

Class A2a: Single or multiple photos (photogrammetry)

In contrast to class A1, the methods of class A2 do not use an image of the heliostat beam on a diffuse target, but instead process a photo of the actual heliostat. The camera is either mounted on the tower or additional masts and either takes a single photo (Röger et al., 2010; Hines and Johnson, 2014; Sauerborn et al., 2013), a series of photos of a moving heliostat (Prahl et al., 2009), or it can be airborne on an unmanned aerial vehicle (UAV) shooting a series of photos of a fixed heliostat from different positions (Jessen et al. 2020).

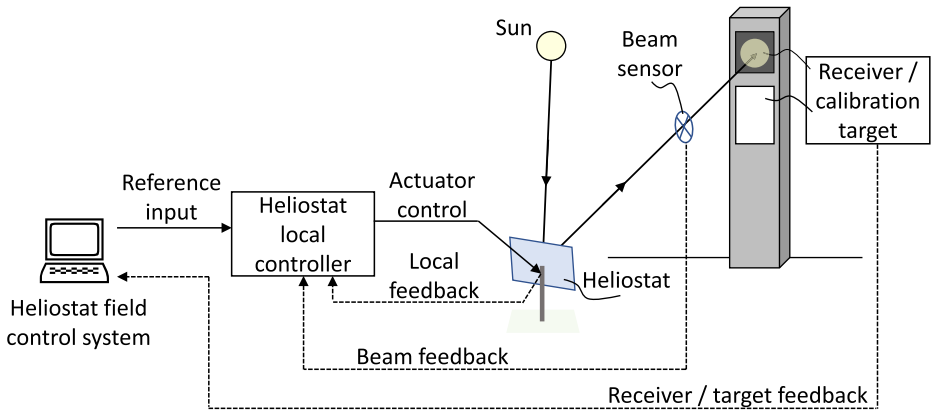

Fig. 5. Illustration of the control signal flows of calibration methods, based on Malan (2014).

Table 2
Criteria to classify calibration systems and resulting classes.

Classification criteria	Classes or variations
Type of measurement signal information (see also Malan, 2014)	• Position of solar focus o on receiver o on calibration target o on sensors, cameras, … • Orientation of reflected beam vector • Orientation of reflecting surface o local feedback (encoder readings, cameras, sensors, …) o remote feedback (measurement of heliostat orientation)
Location, type and number of measuring devices or sensors	• Central camera(s) or sensor(s) (*class A*) o Subclass (A1):Camera(s) on ground – (A1a) Camera-target method using the sun – (A1b) Camera-target method using a signal beam or excitation o Subclass (A2):Camera(s) on tower or UAV – (A2a) Single or multiple photos (photogrammetry) – (A2b) Reflected image of object (e.g. star, LED, sun/sun's brightness distribution) in a heliostat • Central laser or radar based measurement methods (*class B*) o (i) Central laser and cameras o (ii) Central total station o (iii) Central radar o (iv) Central laser scanner • Central solar focus position detection with cameras or sensors on tower *(class C)* o (i) Several cameras or non-optical sensors around receiver o (ii) Several cameras embedded in receiver o (iii) Camera array on moving bar moved along receiver o (iv) Camera array or sensor array as target (iv) • Cameras or sensors on each heliostat (*class D*)
Information density of heliostat surface normals on one heliostat	• Use of normal vector of one point/small surface area on mirror • Use of highly resolved grid of normal vectors distributed over total heliostat mirror surface • Use of a locally mounted measurement device on heliostat
Reference space of calibration	• Calibration of measurement device offset in heliostat surface coordinate space • Calibration of heliostat normal in global tower coordinate system
Accuracy of calibration system	• High accuracy (e.g. for aiming) • Low accuracy (e.g. for directing beam to white target)
Measurement time; applicability to stiff (precise) or soft (imprecise) heliostats; type of control	• Open-loop control, characterisation of heliostat kinematics every few months and storage in heliostat tracking database; slow and applicable only few times per year (months) • Closed-loop tracking control, fast and measuring constantly (seconds)

The method of Röger et al. (2010) relies on an individual image of the heliostat, using automatic edge detection to extract the heliostat and facet vertices as natural markers (see Fig. 9) and derives the heliostat orientation relative to the fixed camera by the ratios of facet side lengths and the angles between observed edges (dimensionless quantities). Hines and Johnson (2014) attach additional diffracting elements on each heliostat. Each diffracting element includes sub-elements producing linear, circular or spiral diffraction patterns. By interpreting the colour or intensity of the reflected radiation, the heliostat orientation can be derived. Prahl et al. (2009) use a series of photos of one heliostat while it is moved around the azimuth and elevation axis. After an automatic edge and vertice detection, a photogrammetric approach delivers the geometry between camera and heliostat vertice orientation from which the heliostat orientation is derived for each photo of the set. Jessen et al. (2020) use an airborne UAV-mounted camera to take photos from more appropriate positions of a non-tracking heliostat. A photogrammetric processing delivers a 3-D point cloud of detected heliostat field features from which heliostat orientations are derived.

The photogrammetric concepts presented in Prahl et al. (2009) and Jessen et al. (2020) should be in the accuracy range between 2 and 6 mrad, hence being deployable for coarse calibration. The concept of Jessen et al. (2020) should yield more precise results due to the more suitable perspectives for photogrammetric evaluation. As merely one image is used, the method of Röger et al. (2010) achieves an accuracy of only between 3 and 10 mrad, depending on the perspective, and is still suitable for coarse calibration. Unlike the others, the concept of Hines and Johnson (2014) should be able to reach fine calibration accuracies, although no information is explicitly given.

Sauerborn et al. (2013) investigated a central camera-based heliostat field calibration method using stereo photogrammetry (see Fig. 10), three coloured markings on the mirror surface and triangulation. The accuracy during the experiments was low (between 48.9 and 172.8 mrad). In a theoretical analysis, a stereo camera system with a resolution of 16 MPixel and distance of 43 m between the cameras is claimed to measure the overall mirror surface normal at an accuracy of 2.27 mrad for a heliostat 50 m away. More details on the described calibration methods can be found in Table 3. The signal flow is shown in Fig. 11.

Class A2b: Reflected image of object (e.g. star, LED, sun/sun's brightness) in a heliostat

Class A2b uses reflected images of an object in the heliostat mirror, e.g. a star (Arqueros et al., 2003; Hines, 2016), an LED (Zavodnya et al., 2015; Prahl et al., 2015), or another object taken by cameras either on the tower or a mast (Arqueros et al., 2003; Hines, 2016; Zavodnya et al., 2015), or from a UAV (Prahl et al., 2015). As the mirror surface is observed directly, no installation or reference calibration of an additional device is required. The heliostats require either a rough pre-calibration in order to view the reflection of the object, a search-and-find procedure moving the heliostat drives or an implementation of intelligent movement of an UAV-mounted camera in the sky. The reflection method has very high accuracies serving as fine calibration. Also, other markers with well-known coordinates in a solar field could be used, such as, for example, the tower edge as proposed by Mitchell and Zhu (2019). Schell (2011) describes an automated and highly parallelised calibration system that was developed by eSolar for its 5 MW_e Sierra SunTower. This calibration system uses multiple towers located around the heliostat field whereby each is fitted with a camera that faces the heliostat field. The cameras are designed such that dozens of heliostats can be simultaneously directed towards and reflect the

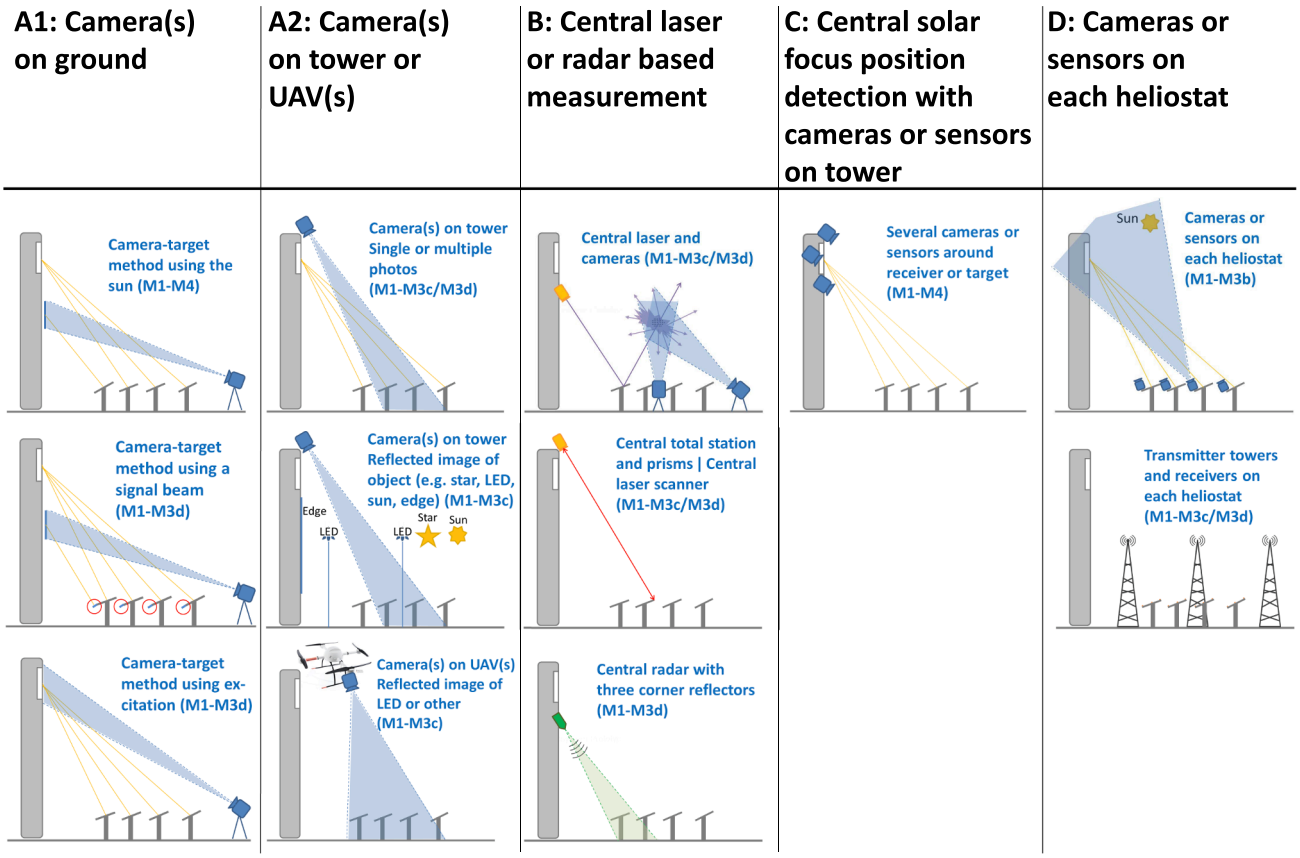

Fig. 6. Visualisation of the resulting calibration system classes according to the classification criterium *Location, type and number of measuring devices or sensors* (Röger et al., 2018) (modified and translated into English).

sunlight directly onto one of the cameras.

The authors estimate calibration uncertainties between 0.1 and 0.3 mrad for these methods, although experiments of Zavodnya et al. (2015) report a value below 1.5 mrad and Arqueros et al. (2003) reports around 1mrad indicating potential for improvement. In the case of measurement during the night, the outlines of the heliostats may not be known accurately, increasing the uncertainty of the calibration. More details on the calibration methods can be found in Table 3. The signal flow is shown in Fig. 11.

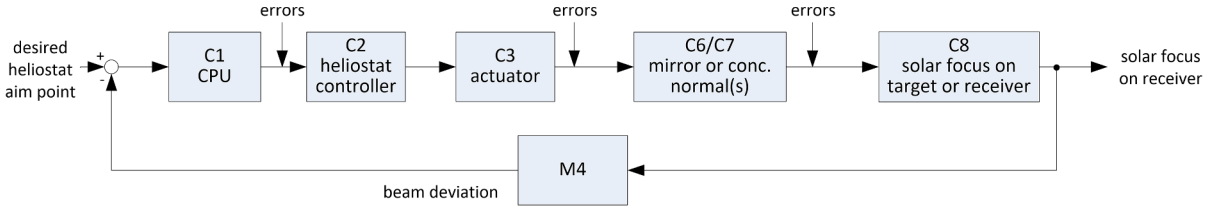

Fig. 7. Signal flow of tracking control methods Class A1 and Class C.

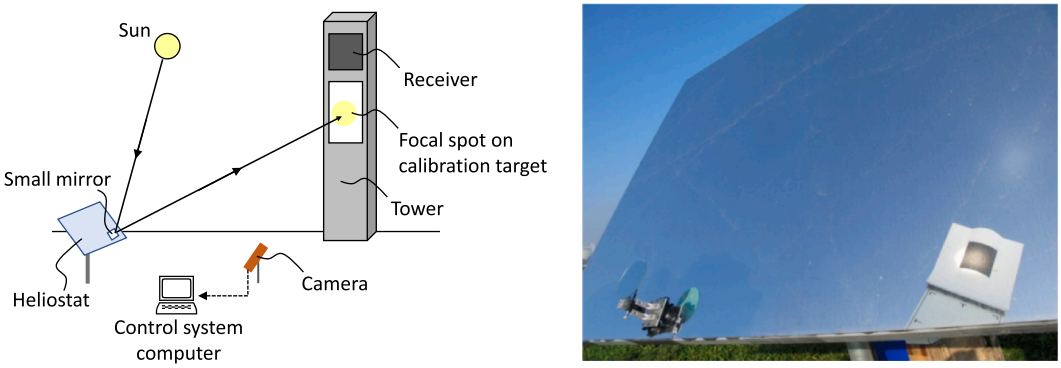

Fig. 8. Illustration of method described by Flesch et al. (2012), Gross (2016) and Belhomme et al. (2011) (left), A small mirror attached to a heliostat at the Solar Tower Jülich as a test setup (right) (Flesch et al., 2012).

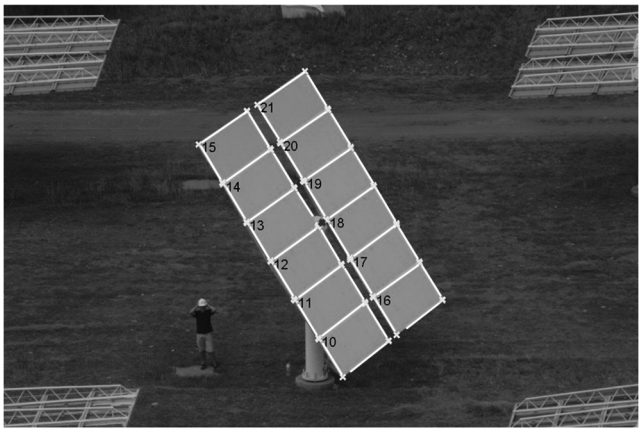

Fig. 9. Image of a photo as example for class A2a (Reprinted from Röger et al. (2010), with the permission of ASME).

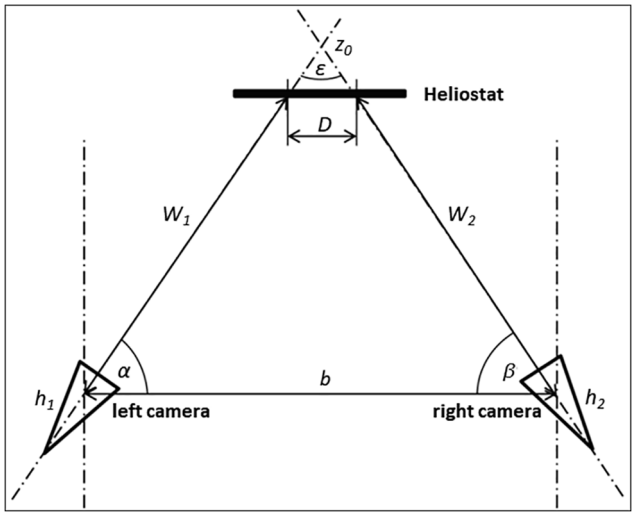

Fig.10. Arrangement of the camera system with view onto a heliostat (Sauerborn et al., 2013), translated to English).

3.2.2. Class B: Central laser or radar based measurement methods

The calibration methods described in this section all measure from a central location at an elevated height such as on the tower of the CRS. Visualisations of these calibration methods are shown in Fig. 6. The signal flow for these methods is shown in Fig. 11. More details on the methods of class B are presented in Table 4.

(i) Central laser and cameras

Dabrowksi et al. (2014) proposed a unique laser calibration system. The calibration system is composed of a laser with high-speed, closed-loop dual-axis tracking system as well as a minimum of two cameras. The calibration process is as follows. The laser is automatically oriented towards a heliostat's mirror facet. When aligned, a short laser pulse is emitted. The mirror reflects the laser beam into the sky and when traversing the near-ground atmosphere, a portion of the laser beam is scattered by molecules as well as aerosol particles in the air. Two or more digital cameras with fitted spectral filters capture the scattered light such that the laser beam becomes visible in an image. The cameras need to be oriented such that the laser beam is viewed from two different angles. By means of image processing, the 3-D vector of the laser beam is calculated from the two images. With the knowledge of the laser source and heliostat coordinates, the normal vector of the mirror facet can then be computed. It is anticipated that with a high laser scanning rate and fast image processing, an entire heliostat field can be calibrated in quasi-online mode in short time intervals of a few minutes. First experiments in a laboratory environment showed that the method works. An impulse laser with a central wavelength of 355 nm and beam outlet diameter of about 50 mm was used at the Solar-Institut Jülich (details to be published). Images of the scattered laser beam were acquired with a scientific, ultraviolet-sensitive camera with interline CCD sensor as well as an image intensifier camera. This calibration method still requires proof of concept in field tests which are due to be carried out.

(ii) Central total station

A concept for the calibration of heliostats with a central total station is to deploy an automated total station, mounted in a central position such as atop of the power tower, for automatically surveying the position respective to the orientation of the heliostats with the help of prisms. The total station, respectively the post processing software, detects mounted prisms on each of the heliostats, calculates the normal vector of the prisms' plane and the offset from the desired orientation. Each heliostat must be equipped with at least 3 standard glass triple prisms which are best mounted to the heliostat structure during the assembly process. It is essential that the prisms' plane accurately fits the mirror or concentrator plane (same normal vectors). Alternatively, the alignment of the prisms can be measured during the pre-calibration process. To avoid irritations of the scattered light of the receiver, the measurement can also be executed at night or at times when the heliostats are not focussing. Prior to the measurement, the heliostats need to be roughly oriented towards the total station to ensure the detection of the prism. Depending on the field of view and the size of the heliostat field, either one or more total stations are required.

(iii) Central radar

Sauerborn et al. (2012) describe a patented heliostat field calibration method based on the use of high-frequency, high-resolution millimetre wave working on the principle of radar inverse synthetic aperture radar (ISAR). Each heliostat needs to be equipped with at least three corner reflectors, as shown in Fig. 12 (left), which form a plane from which the overall heliostat frame normal can be determined. For a scan of a heliostat field the three corner reflectors of each heliostat must be in view for all possible tracking angles throughout the day. For conducting the experiments, the radar was installed at a height of about 30 m on the tower as illustrated in Fig. 12 (middle). Furthermore, the radar must be moved linearly along a rail during a scan. This allows a variation in range to be detected from the measured coherent phase information, resulting in an azimuthal resolution of a heliostat's orientation. Fig. 12 (right) depicts an image of the detected three corner reflectors of a small group of five heliostats. In an extensive field

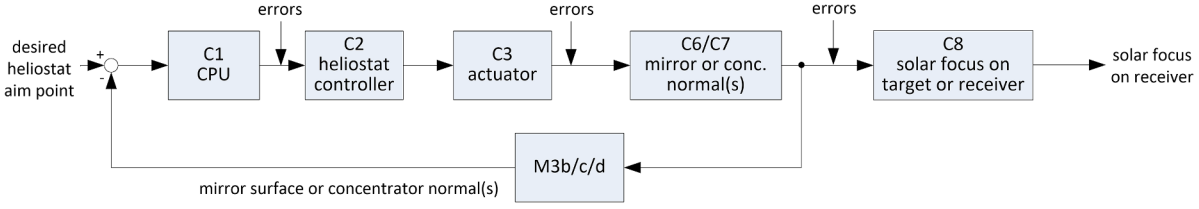

Fig.11. Signal flow of tracking control methods Class A2, Class B and Class D.

experiment, larger heliostat field sections at the Solar Tower Jülich (STJ) comprising about 100 heliostats with distances between 50 and 300 m from the tower were scanned. Further optimisation steps are necessary to achieve the desired maximum attainable accuracy of about 2 mrad.

(iv) Central laser scanner

Sauerborn et al. (2013) investigated a heliostat field calibration method based on laser scanner technology. Fig. 13 shows the result of a surface scan of the backside of a heliostat. The backside was chosen because the quality of signal detection would be too low if the reflecting mirror front was chosen. Generally, with greater measurement distances the quality of signal detection strongly reduces. However, the required location of the laser scanner facing the back of the heliostats leads to an unfavourable view angle that only allows a few heliostats being scanned. Hence, this method for this measuring system is not practical. Laser scanning methods whereby the scanner faces the heliostat mirror facets are also discussed but were not evaluated in experiments. A frontal scan requires, for example, the permanent mounting of reflector foils, other detectable objects or the application of a diffuse reflecting material whereby the latter is not used during the regular heliostat field operation.

3.2.3. Class C: Central solar focus position detection with cameras or sensors on tower

The calibration methods of class C all have cameras or sensors fitted centrally on the tower. Visualisations of the methods are presented in Fig. 6. The signal flow is shown in Fig. 7. More details on the class C methods are presented in Table 4.

(i) Several Cameras or Non-Optical Sensors around Receiver:

A calibration method by Yogev and Krupkin (1999) requires the installation of four cameras around the receiver, as illustrated in Fig. 14 (right), to measure a heliostat orientation by means of comparing the brightness differences in an image with image processing software for each mirror seen by each of the four cameras. An important criterion is that all four cameras are synchronised and have the same time stamp. A simplified example of a measuring process is shown in Fig. 14 (left), where three heliostats are in the field of view of each camera. The example demonstrates for a single, central aim point on the receiver, that the heliostats labelled 'H2' and 'H3' are accurately aligned as the mirror brightness for the two heliostats is identical in all four images. On the contrary, the heliostat labelled 'H1' is vertically accurately aligned, but horizontally misaligned which is indicated by the mismatch in mirror brightness between the left and the right camera.

A first demonstration of the calibration method was presented by Kribus et al. (2004) which is based on the principle of Yogev and Krupkin (1999). It should be noted that Yogev was co-author of this publication. Fig. 15 shows images from experiments for heliostats photographed from a far and near distance from the target centre.

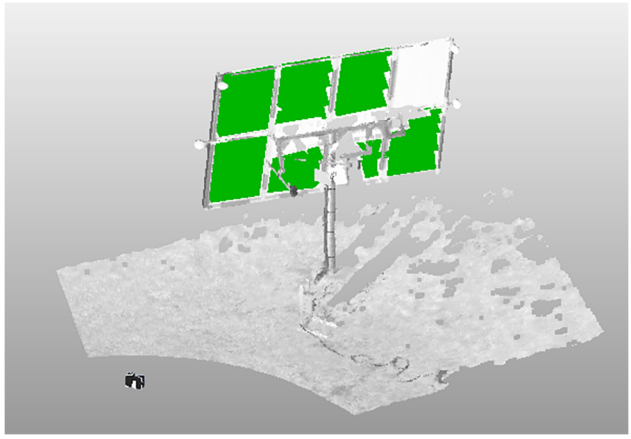

Fig. 13. 3-D visualisation of the measured heliostat with orientation measurement via various marked regions on the mirror backside (area detection) by Sauerborn et al. (2013).

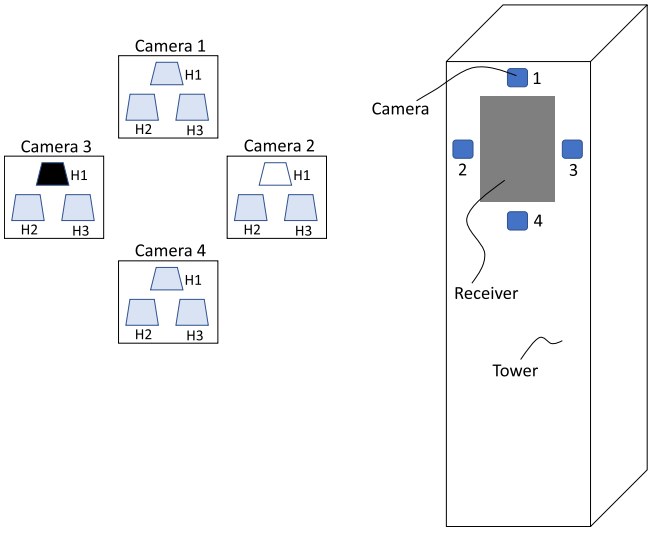

Fig. 14. Simplified example of a measuring process where three heliostats are in the field of view of each camera (left). Concept of the front view of the receiver with four cameras around it (right), as proposed by Yogev and Krupkin (1999).

Koningstein et al. (2012) patented a method which appears to be very similar or identical to the one of Yogev and Krupkin (1999).

Coquand et al. (2017) produce an overlay of images of 4 cameras and determine the differences in the 4 images to correct the errors of single heliostats. Convery (2011) uses mechanical vibrations on the heliostat facets to identify them with photosensors surrounding the receiver target via the time-dependent changes in the wavefront of the

Fig. 12. Exemplary measuring scene of five heliostats equipped with three corner reflectors at the Solar Tower Jülich (STJ) (left), Position of radar on the research platform of the STJ (middle), Processed SAR image of heliostat field with five heliostats in the centre, each is equipped with three corner reflectors (right) (Sauerborn et al., 2012).

reflected light. Outdoor testing was done with a small-scale model consisting of one mirror and 4 photosensors. In a patent by Convery (2013) using sensors, two designs were described (cf. Fig. 16).

Freeman et al. (2015) mount piezo-electric actuators on the heliostat facets and detect misaligned heliostats with photo-sensors around the receiver. The identification of a single heliostat is established by analysing the oscillating wave front by applying FFT.

(ii) Several Cameras embedded in Receiver:

Goldberg et al. (2015) mounted a pinhole camera (camera obscura) in a gap between receiver pipes and monitors the semi-transparent screen on the backside with a CCD-camera. The method foresees that a few cameras are embedded inside a receiver such that the heliostat field can be consistently monitored. Not intended as a traditional alignment calibration system, this method is described as a system to estimate flux maps on the receiver during solar operation. By means of image post-processing, the flux impinging on a camera's position as well as the flux contributed by each individual heliostat in the field can be determined amongst other features. The system also allows the online assessment of the heliostat alignment accuracy (the paper states: "*supporting a heliostat calibration system, and a potential alternative to that system*"). Two types of estimations are used: the estimation of the error variance as well as error bias that lead to a better estimation of the expected flux maps on the receiver. The latter is also used for correcting the error bias.

(iii) Camera Array on Moving Bar moved along Receiver:

Collins et al. (2017) suggest a camera array moving across the receiver. A proof-of-concept is demonstrated with one camera and four heliostats. Fig. 17 (left) shows the concept design of the calibration system with the camera array on a moving bar as well as an example of camera images obtained from image acquisition during sweep. Fig. 17 (right) shows a real camera image when four heliostats were aimed at a camera in a proof-of-concept experiment. The heliostat field calibration method shall be capable of closed-loop heliostat control and lead to reduced costs of the heliostat control system.

(iv) Camera Array or Sensor Array as Target:

Gross (2016) foresees, amongst other, the possibility of evaluating signal beams using an array of digital cameras, optical sensors or photodetectors as target (e.g. underneath the receiver), as shown in Fig. 18.

3.2.4. Class D: Cameras or sensors on each heliostat

Calibration systems capable of closed-loop tracking control of type Class D are based on a camera or optical sensor attached to the moving reflector part of the heliostat. The actual orientation of the reflector is determined via object recognition in the camera image based on known objects in space. Although, in principle, the camera can be oriented in any orientation, two main approaches are described so far:

- Camera attached forward facing
  - o detection of sun position in camera image
  - o detection of other reference point(s) in camera image (typically the tower, the receiver or a target)
  - o great difference in brightness of objects (e.g. sun and target), can be dealt with by appropriate filters and different exposure time
- Camera on reflector backside
  - o evaluation of reflector orientation based on several (at least 2) known objects in the field of view

Both methods require an initial as well as periodic calibrations from time to time (to determine the camera position and orientation relative to the reflector). Using such a system for heliostat calibration implies that during the calibration process a correlation is determined between the camera-based result and other tracking control devices, typically angle sensors or step counters on the drives of the two rotation axes of the heliostat. Tracking is then performed using the tracking control devices, and the correlation is checked and eventually updated by regular calibration measurements.

Recent developments tend to use the camera-based calibration method directly for tracking control, thus avoiding the need for additional tracking control devices and leading to further cost reduction. With modern low-cost hardware, image recognition has become sufficiently fast and accurate such that the calibration and tracking control can be performed by the controller of each heliostat. Class D methods feed the signal from M3b back to M1 as indicated in Fig. 11.

Pfahl et al. (2009) filed a patent for a calibration system capable of closed-loop tracking control based on a camera mounted on the front side of a heliostat reflector (cf. Fig. 19). The camera continuously captures images from the sun and from a second object in the field of view, e.g. the receiver. The orientation of the heliostat reflector is determined using image recognition of the sun and the second object based on the known coordinates of the sun (sun position calculated via sun position algorithm, use of second object's position with known coordinates in the fixed coordinate system). The patent describes several implementation options, as for example the use of different

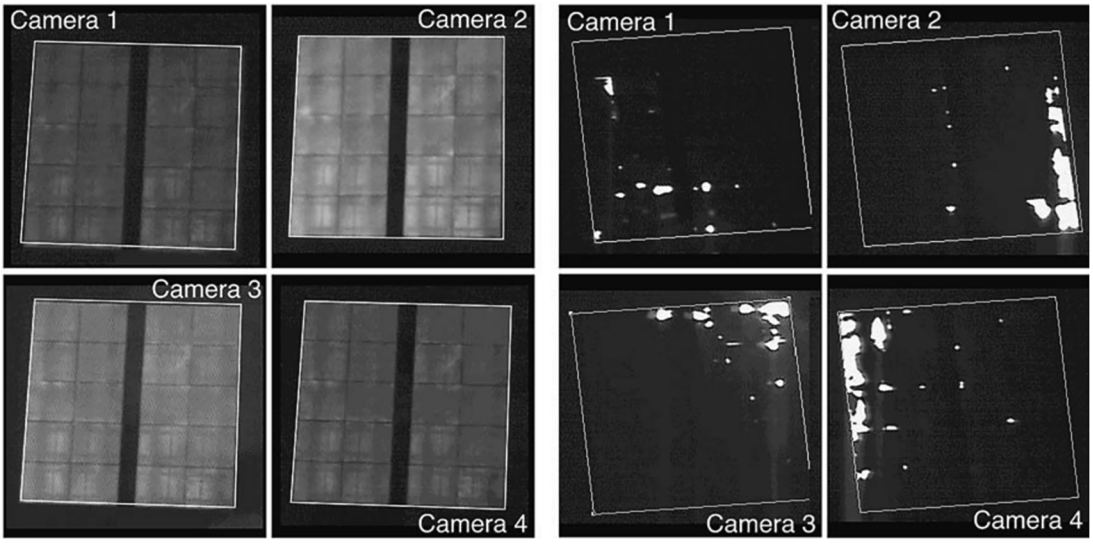

Fig. 15. Images acquired for a single heliostat that is far away from the target centre (left), and when nearer the target centre (right). The heliostat's edges were detected and added by the software (Kribus et al., 2004).

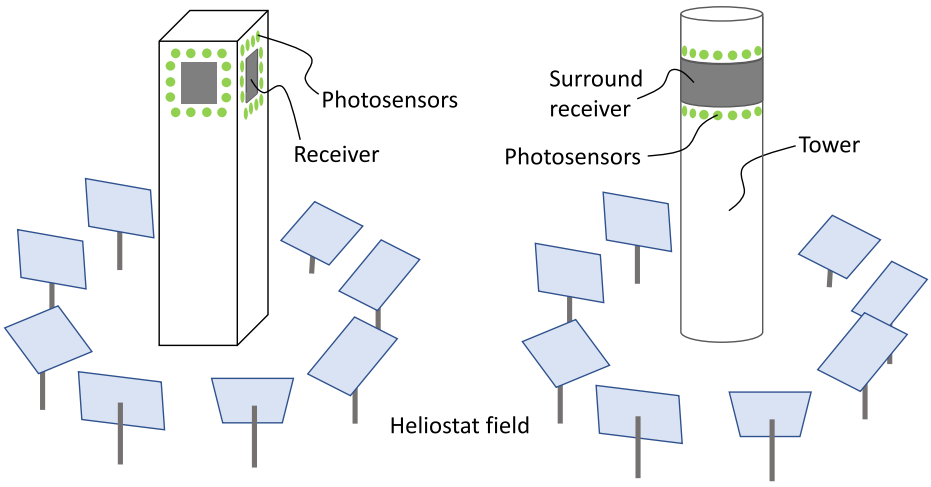

Fig. 16. Illustration of the arrangement of photosensors at the receiver edges shown for two receiver types, as proposed by Convery (2013).

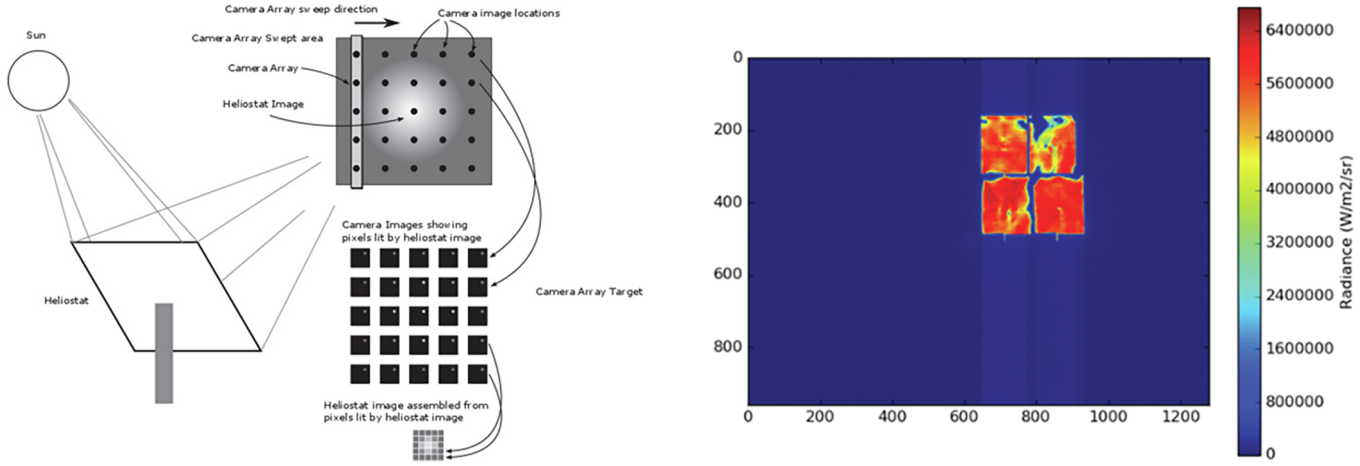

Fig. 17. Concept design of calibration system with camera array on moving bar and example of camera images obtained from image acquisition during sweep (left), Real camera image obtained in a proof-of-concept experiment (right). Reprinted from Collins et al. (2017), with the permission of AIP Publishing.

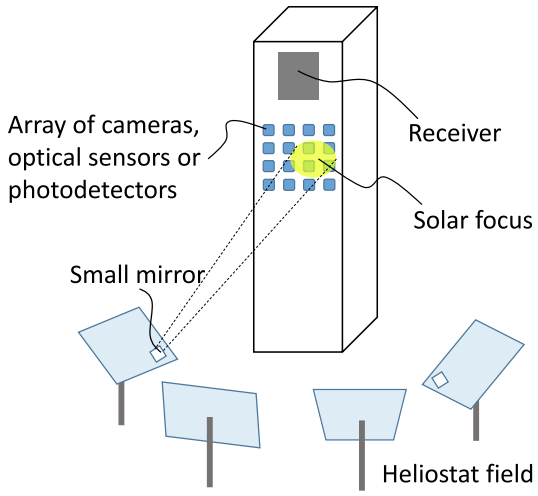

Fig. 18. Illustration of method from Gross (2016) showing signal beams reflected onto an array of digital cameras, optical sensors or photodetectors below the receiver.

exposure times to capture the sun and the second object in two separate consecutive images in order to obtain better image recognition results, the use of artificial passive or active markers (e.g. light emitting diodes) as well as the use of spectral filters. In the reference the method is described in more detail, but results from a real implementation are not reported. A first implementation of this system is described by Pfahl et al. (2019) as work in progress with results pending. The minimum required components are: one camera on each heliostat with a corresponding processing unit. Hickerson and Reznik (2012) patented a similar system for a heliostat with integrated image-based calibration system capable of closed-loop tracking control. They broadened the scope of the idea by claiming specific filtering options, e.g. locally adaptive filtering for the view range of the sun.

Fairman et al. (2019) investigated a closed-loop optical tracking method based on an array of retroreflectors mounted near the receiver, which are viewed by a camera mounted to each heliostat, as shown in Fig. 20 (left). The position of the sun image at the receiver can be determined with a sufficient number of retroreflectors located in the vicinity (or in front) of the receiver. The incident sun rays from a heliostat that impinge on one or more retroreflectors are reflected back to the heliostat. The camera of each heliostat captures an image. With image processing, the orientations of the heliostats are evaluated from the

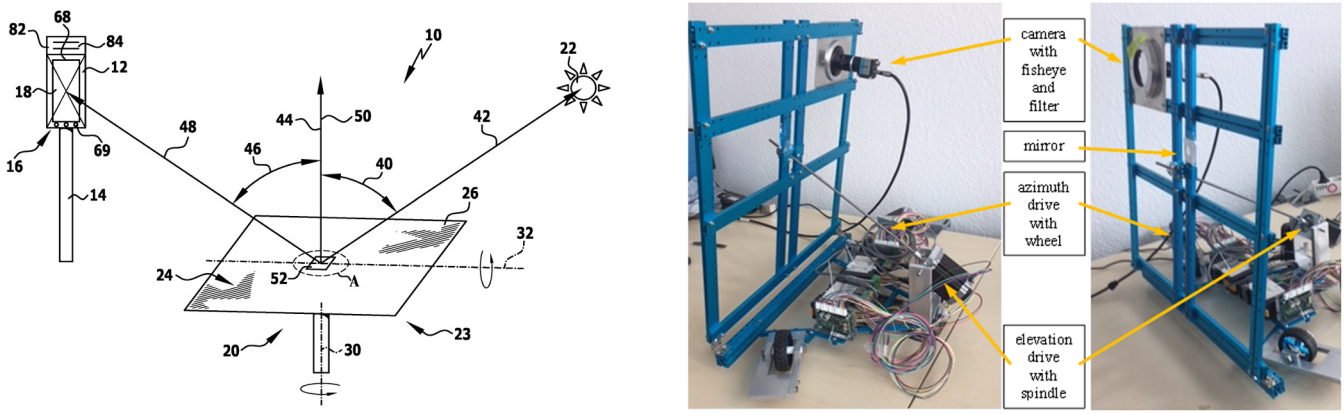

Fig. 19. Camera-based tracking control using sun and receiver (Pfahl et al., 2009) (left), Implementation of calibration system (right). Reprinted from Pfahl et al. (2019), with the permission of AIP Publishing.

reflected, relative brightness of the retroreflector arrays. A trial was conducted with a simplified target with five retroreflector, as shown in Fig. 20 (right). Such a calibration method is patented by Koningstein (2012).

Burisch et al. (2018a) investigated and successfully tested a method for the automatic calibration of a heliostat field by means of equipping each heliostat with a camera which must have targets with known locations in its field of view, such as lights, the sun or the moon. The method is called *Scalable HeliOstat calibRation sysTem (SHORT)*. This calibration method allows all heliostats to calibrate themselves automatically and independently from each other. Fig. 21 shows details of the mounted camera and artificial light sources as targets. With the SHORT method, the heliostat axes orientation as well as the actual kinematic model can be computed for each heliostat (Sánchez, 2018). Further information on the system is given, such as that the light sources must be easily detectable and preferably of spherical shape, that the cameras can be mounted in any orientation and location on the heliostat and that the artificial targets can be placed atop of poles and on the tower. The accuracy from the field tests is stated as 0.6 mrad. Information on the issued patent can be found in the reference (Sánchez González et al., 2017).

Harper et al. (2016) investigated the use of MEMs and optical sensors for closed-loop tracking control which also included combining the equipment as well as a simple machine learning approach. Initial experiments were carried out with a mobile phone with onboard sensors (including a camera, 3-D capable accelerometer, gyro and compass) mounted on a heliostat in a rear facing position. Two types of targets are presented. Test results showed that the highest accuracy is obtained when solely the optical sensor (i.e. camera) is used. The stated accuracy for the calibration method using the camera is 0.9 mrad (mean) at a sensor resolution of 2592 × 1944 pixels. The use of the accelerometers showed insufficient accuracy in the range of 10 mrad.

van den Donker et al. (2016) describe a method for closed-loop tracking control based on attaching an optical sensor, an acceleration sensor and a magnetic sensor on each heliostat. The optical sensor is mounted on the mirror. With the sun position in the field of view, the angle of incidence of the sun position with respect to the normal (or axis) of the mirror can be measured. The difference in azimuth angle between the direction of the sun and the mirror's optical axis is calculated from the angle of incidence, measured by the optical sensor, and the elevation angle of the optical sensor, measured by the acceleration sensor. The accuracy of the optical sensor from laboratory testing is stated to be 0.13 mrad (3σ) and 0.15 mrad (3σ) for the accelerometer. The magnetic sensor is used solely for determining the azimuth angle during a night-time calibration. It was found to be less accurate but no definite value was stated. As it is used only during cloudy weather and at night the lower accuracy has less impact.

Swart (2017) describes a method with three or more receiver sensors attached to the heliostat mirror surface that receive radio-frequency signals from several transmitter towers located around the heliostat field (cf. Fig. 22). The arrangement of the receivers is such that they are used to define a plane on the heliostat surface from which a heliostat normal is calculated. The signals from the transmitter towers are received by each of the three or more receivers. The signals are processed using the principle of electronic phase delay and the phase delay due to the distance from the transmitter towers. The position of points R_1 to R_r are computed by measuring the distance between each receiver and the transmitters T_1 to T_i. Simulation results showed that an aiming accuracy error ≤ 1 mrad can be realised. A fully functioning prototype system setup would require a minimum of 5 transmitters and

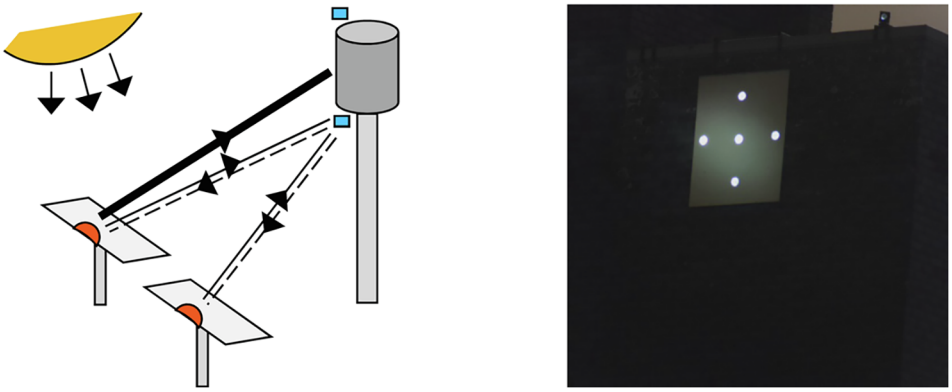

Fig. 20. Schematic of system's working principle (left). Image of a simplified target with five retroreflectors captured by a camera mounted on a heliostat during a trial (right). Reprinted from Fairman et al. (2019), with the permission of AIP Publishing.

Fig. 21. Heliostat with mounted camera viewing an artificial light target on a tower during calibration (left), View of an artificial light target as seen by a camera mounted to a heliostat (right). The targets as well as camera are highlighted with red circles. Reprinted from Burisch et al. (2018a), with the permission of AIP Publishing.

3 receivers, which must all be installed with a precision in the sub-millimetre range. Additionally, but centrally located, electronics for modulation and demodulation are needed.

Carballo et al. (2019) describe the application of deep learning algorithms for the object recognition in the camera image using low-cost camera and processor hardware. The new aspect is the use of a neural network method known as Faster R-CNN. A prototype system was installed on a heliostat and tracking tests were conducted. First, the neural network had to be trained using a large number of images taken over the complete viewing range. The system was trained for the detection of sun, target, clouds and surrounding heliostats. With a commodity-type microcomputer and an 800 × 600 Pixel camera, the authors report a tracking accuracy of less than 3 mrad under normal conditions. The authors claim that with improved hardware the tracking accuracy could be easily increased. The minimum required components are: one camera on each heliostat with a corresponding processing unit.

Sauerborn et al. (2013) investigated a heliostat field calibration method based on the use of inclinometers and magnetic encoded sensors installed on heliostats as shown in Fig. 23. Note that this calibration method is referred to as reference [S13b] in Table 4.

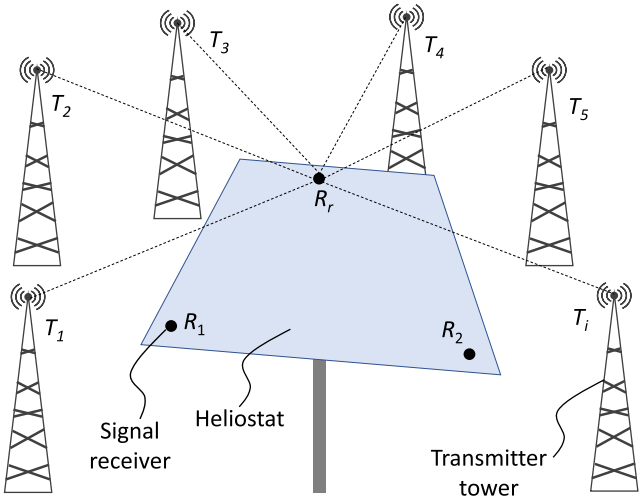

Fig. 22. Method with three or more signal receivers mounted on a heliostat and several transmitter towers around the heliostat field (own drawing, based on Swart (2017)).

3.3. Characteristics of calibration methods

Table 3 and Table 4 summarise the key data on the abilities of the calibration methods as per class. If available, published data from the stated literature was used but it has not been experimentally contrasted or validated by the authors. When data was unavailable (e.g. for the case of patents), the authors made estimates based on their own experience and clearly indicated when a value is an estimate (E). For some instances, marked with (E), the authors made estimates that are better than values stated in literature based on own experience or technology advancements since the publication of the described calibration method. The stated values should be viewed as being indicative or an approximation but not be used for performing a rigid comparison between all the calibration methods. Some calibration methods that appear to be identical to others may have been omitted in the tables for ease of reading. This includes, for example, results presented in a publication for a method that is based on a patent. The calibration methods cover a wide range of technology readiness level whereby some may have merely been tested in a laboratory environment for proof-of-concept purposes, while others have been experimentally tested and validated in a real heliostat field. Therefore, the stated data must be viewed critically.

Fig. 23. Example of an inclinometer for the measurement of the inclination (left), and magnetic encoded sensors for both azimuth and zenith orientation measurement (right) (Sauerborn et al., 2013).

Table 3
Key data on selected calibration methods: Single camera or sensor on ground/tower/UAV (class A).

	Class A1: Camera on ground		**Class A2: Camera on tower or UAV**	
	Class A1a Camera-target method using the sun	**Class A1b** Camera-target method using a signal beam or beam excitation	**Class A2a** Single or multiple photos (photogrammetry)	**Class A2b** Reflected image in a heliostat of star, LED, sun/sun's brightness or object
Coverage of the signal chain (see. Fig. 2)	**M1 – M4**	**M1 – M4 (excitation)** **M1 – M3d (signal beam)**	**M1 – M3c/M3d**	**M1 –M3c**
Measurement process				
(1) Accuracy	~0.1 mrad **E**	~0.2 mrad (estimated) **E**	[R10] ~ 3–10 mrad [H14] ~ 0.2–5 mrad **E** [P09] ~ 2–6 mrad [Q20] ~ 2–5 mrad **E** [S13] < 2.27 mrad **E**	[Z15,H16,M19,Q21] ~ 0.1–0.3 mrad **E** (reported: < 1.5 mrad); [Sc11] ~ 0.1–0.3 mrad **E** [A03] 1 mrad
(2) Number of normal vectors per heliostat[1]	1	1	[R10,P09,Q20] corresponds to number of detected mirror panels; [H14] corresponds to number of diffraction patterns; [S13] 1	[Z15] 1 (if heliostat not moved); [Q21] several (depending on flight route); [A03,H16] several (depending on measurement time; position change of stars visible in mirror facets depends on earth rotation velocity)
(3) Time per measurement process per heliostat	~20 s (depending on speed of heliostat movement) **S**	[B16] ~ 40 s **S/G,E;** [G15,F12] ~ 20 s **S/G,E**	[P09]: ~0.5 h **S/G;** [Q20]: ~60 s **G**; [R10,H14]: 1 s **S/G,E;** [S13] < 1–3 s **S,E**	[Z15] ~ 1 s **S/G,E;** [Q21] ~ 1 s, **G,E;** [A03,H16] for one normal vector: seconds; for several vectors: minutes **S/G,E**
Possible applications				
(4) Reference calibration necessary[2]	no	[B16] no; [G15,F12]: yes	[R10,P09,Q20,S13] no; [H14]: yes	no
(5) Calibration in GCS [3]	yes	yes	yes	yes
(6) Pre-calibration (coarse calibration)[4]	only with focus scanning	no	[R10,P09,Q20,S13]: yes; [H14]: prior rough alignment may be necessary	[Z15,A03] no, tower must be ready and good alignment; [Q21] in principle yes, but practically no
(7) Regular calibration (fine calibration) and OCS capability[5]	RC yes, but prior rough alignment necessary; OCS no	[all] RC yes, but prior rough alignment necessary; [B16] OCS yes, but perhaps only for limited number of heliostats **E**; [G15,F12] OCS no	[H14] RC yes; [others] RC no; [H14] OCS yes, but perhaps only for limited number of heliostats **E**; [others] OCS N/A	[all] RC yes; [all] OCS no **E**
Operational requirements and limits				
(8) Tolerable degree of soiling	high	high	medium	low
(9) Requirements for meteorological conditions	sun	sun	ambient light; [H14] condensate / rain may disturb	sun or night without condensate on mirror

(*continued on next page*)

Table 3 (*continued*)

	Class A1: Camera on ground		Class A2: Camera on tower or UAV	
	Class A1a Camera-target method using the sun	**Class A1b** Camera-target method using a signal beam or beam excitation	**Class A2a** Single or multiple photos (photogrammetry)	**Class A2b** Reflected image in a heliostat of star, LED, sun/sun's brightness or object
(10) Measurable heliostat orientations	all	all	Extreme angles to camera difficult to measure **E**; [R10,P09,Q20,S13]: small elevations maybe difficult	Some limitations regarding constellation camera to star/LED/object and ground reflections
(11) Restrictions in measurable heliostat location	distant heliostats difficult to measure	distant heliostats maybe difficult to measure **E**	distant heliostats maybe difficult to measure **E**	none
(12) Restriction in measurable heliostat sizes	distant & small heliostats difficult	none	none	none
(13) Restrictions in measurable heliostat geometries	none	none	none **E**	none **E**

Legend

[B16]	Bern et al. (2016)	[R10]	Röger, Prahl and Ulmer (2010)	[Q20]	Jessen et al. (2020)	[Q21]	Prahl et al. (2015)
[G15]	Gross (2016)	[H14]	Hines and Johnson (2014)	[Z15]	Zavodnya et al. (2015)	[H16]	Hines (2016)
[F12]	Flesch et al. (2012)	[P09]	Prahl et al. (2009)	[A03]	Arqueros, Jimenez and Valverde (2003)	[M19]	Mitchell and Zhu (2019)
[S13]	Sauerborn, Göttsche and Hoffschmidt (2013)	[Sc11]	Schell (2011)				

E Estimated value by authors, **P** Parallel calibration process (simultaneous calibration of all heliostats), **S** Sequential calibration process (calibration of one heliostat after another), **G** Group of heliostats that can be calibrated simultaneously (max. number of heliostats in a group depends on capability of calibration system).

[6] Number of normal vectors that can be measured per heliostat (this is specifically important for heliostats with multiple facets).

[7] Measurement of the orientation of the measurement device, data processing and derivation of correction values for the device orientation in the heliostat coordinate system. This is subsequently followed by an implementation of the correction values in the control system (This type of measurement is only required for calibration systems that either deploy a measurement device for each heliostat or if only one mirror point is used).

[8] Measurement, data processing and derivation of correction values for the heliostat (facet's) normal orientation in the global coordinate system (GCS). This is subsequently followed by an implementation of the correction values in the control system (Required in any case whether a measurement device for each heliostat is deployed or not).

[9] Coarse calibration during construction phase with accuracy of around 3 to 10 mrad. Hardly any previous knowledge/infrastructure available.

[10] Accuracy around 0.1–0.3 mrad. The acronyms RC and OCS refer to Regular Calibration and Online Calibration System, respectively.

Table 4
Key data on selected calibration methods: Classes B, C and D.

	Class B Central laser or radar based measurement methods	**Class C** Central solar focus position detection with cameras or sensors on tower	**Class D** Cameras or sensors on each heliostat
Coverage of the signal chain (see. Fig. 2)	**M1 – M3d**	**M1 – M4**	**M1 – M3b**
Measurement process			
(1) Accuracy	(i) [Da14] To be determined (ii) 1.1 mrad and 0.42 mrad for a 15 m^2 and 100 m^2 heliostat, resp.** (iii) [S12] 2 mrad **E** (iv) [S13] 2 mrad (precision)	(i) [K04] ~ 0.1–0.3 mrad [6] (i) [Cq17] ~ ≤ 0.3 mrad **E** [6] (i) [Cy11] ~ ≤ 0.3 mrad **E** [6] (i) [Fr15] ~ ≤ 0.3 mrad **E** [6] (ii) [Gb15] ~ ≤ 0.3 mrad **E** [6] (iii) [Cs17] ~ ≤ 0.3 mrad **E** [6] (iv) [G15] ~ 0.2 mrad **E**	[B18a] 0.6 mrad (rms) [7] [Ha16] 0.9 mrad (mean) [7] [Fm19] < 1 mrad [7] [D16] 0.13/0.15 mrad (3σ) [Cb19] < 3 mrad [7] [HK19] No value stated [Sw17] < 1 mrad (simulated) [S13b] No value stated
(2) Number of normal vectors per heliostat[1]	1	1	1
(3) Time per measurement process per heliostat	(ii) [Da14] < 1 s **E,S;** [S12,S13] ~ 30 s **G,S,E;**	[All, except G15] ~ 10–120 s **E,P;** [G15] ~ 1–10 s for camera array **E,P**	< 1 s **E,P**
Possible applications			
(4) Reference calibration[2]	no	yes	yes
(5) Calibration in GCS [3]	yes	yes	yes
(6) Pre-calibration (coarse calibration)[4]	yes, with coarse alignment in direction of measuring device	no	Yes
(7) Regular calibration (fine calibration) and OCS capability[5]	(ii) depends on distance and size of heliostat, [S12,S13] RC no; [all] OCS no	[all]: RC yes; [all]: OCS yes	[B18a,Ha16,D16,Sw17]: RC yes; [Cb19,S13b]: RC no (in current version); [B18a,Ha16,D16,Sw17]: OCS yes; [Cb19]: OCS no
Operational requirements and limits			
(9) Tolerable degree of mirror soiling	Probably high	High	Low-medium
(10) Requirements for meteorological conditions	[S12] none; [others]: no dew and no fog	Sun	None[B18a,Ha16,Sw17,Cb19,S13b], daylight[D16, Cb19], sun[D16,Cb19]
(11) Measurable angularity of heliostat orientation	No extreme angle positions in relation to measuring device	Near-target	Any
(12) Restrictions in measurable heliostat location	Depends on devices' specifications	None	None
(13) Restrictions in measurable heliostat sizes	None	None	None
(14) Restrictions in measurable heliostat geometries	None	None	None

Legend

[K04]	Kribus et al. (2004)	[Cq17]	Coquand et al. (2017)	[G15]	Gross (2016)	[D16]	van den Donker et al. (2016)
[Gb15]	Goldberg et al. (2015)	[Cs17]	Collins et al. (2017)	[B18a]	Burisch et al. (2018a)	[Cb19]	Carballo et al. (2019)
[Cy11]	Convery (2011)	[Fr15]	Freeman (2015)	[Ha16]	Harper et al. (2016)	[Hk12]	Hickerson and Reznik (2012)
[Sw17]	Swart (2017)	[S12]	Sauerborn et al. (2012)	[S13]/[S13b]	Sauerborn et al. (2013)	[Da14]	Dabrowksi et al. (2014)
[Fm19]	Fairman et al. (2019)						

E Estimated value by authors, **P** Parallel calibration process (simultaneous calibration of all heliostats), **S** Sequential calibration process (calibration of one heliostat after another), **G** Group of heliostats that can be calibrated simultaneously (max. number of heliostats in a group depends on capability of calibration system).
**Example for a total station with 1.8 mm distance measurement error and 2.4 mm angle measurement error (0.15° angle measurement accuracy). Accuracy depends on distance and size of heliostat. Calculation example for square shaped heliostat at a distance of 1000 m.

[6] Number of normal vectors that can be measured per heliostat (this is specifically important for heliostats with multiple facets).

[7] Measurement of the orientation of the measurement device, data processing and derivation of correction values for the device orientation in the heliostat coordinate system. This is subsequently followed by an implementation of the correction values in the control system (This type of measurement is only required for calibration systems that either deploy a measurement device for each heliostat or if only one mirror point is used).

[8] Measurement, data processing and derivation of correction values for the heliostat (facet's) normal orientation in the global coordinate system (GCS). This is subsequently followed by an implementation of the correction values in the control system (Required in any case whether a measurement device for each heliostat is deployed or not).

[9] Coarse calibration during construction phase with accuracy of around 3–10 mrad. Hardly any previous knowledge/infrastructure available.

[10] Accuracy around 0.1–0.3 mrad. The acronyms RC and OCS refer to Regular Calibration and Online Calibration System, respectively.

[11] For methods of types (i), (ii) and (iii) the accuracy can be regarded as being (nearly) identical to the global tracking error as the entire heliostat's mirror surface is evaluated to a high degree of accuracy.

[12] The stated accuracy is the overall heliostat tracking accuracy;

4. Assessment

This chapter addresses the advantages and disadvantages associated with the calibration methods of classes A to D. However, it is not possible to reliably and fairly assess or rate calibration systems with respect to establishing a ranking. This is due to the varying technical readiness levels (e.g. patent only, publication of laboratory test results, publications with validated field test results, commercial readiness) as well as the lack of published data and independent verifications. Despite having stated that a reliable ranking cannot be realised, the authors give their own opinions.

4.1. Advantages and disadvantages of the calibration methods

4.1.1. Subclass A1: Camera(s) on ground

Class A1a: Camera-target method using the sun

Advantages:

The camera-target method is currently the state-of-the-art method with the largest track record, delivering very accurate heliostat orientation data with accuracies around 0.1 mrad (fine calibration) but only if the heliostat movement is reproducible. The camera-target method uses a simple setup with relatively low-tech components, i.e. a white Lambertian target, a camera and a computer for image processing. Measuring an individual heliostat's solar focus directly on the target (M4, see Fig. 2) delivers a highly accurate feedback signal, but the method cannot be used for closed-loop tracking control as it is too slow and does not work on the receiver.

Disadvantages:

The drawback is that with a high number of heliostats, the calibration process needs a lot of time. This is due to the reason that it is necessary to slew each heliostat away from the receiver onto the target sequentially because otherwise the heliostat images on the target would interfere with one another. Additionally, the elevation and azimuth angles which can be calibrated depend on the point of time in the year because the sun is used. Furthermore, there is certain initial effort necessary for a coarse pre-calibration of the heliostats to focus on the calibration target. Heliostats far away from the target or very small ones may not deliver sufficient contrast on the target and are more difficult to measure. Soft or imprecise heliostats will have a lower accuracy with this method. The method can only be applied during sunny periods with direct solar irradiance or during full moon.

Class A1b: Camera-target method using a signal beam or beam excitation

General advantages:

The main advantage of using a signal or an excited beam is that the individual heliostat beams can be recognised, even if there is superposition of the main beams. This opens up the horizon to calibrate several heliostats in parallel, or even to implement a closed-loop tracking control, if there is enough space for the signal beams on a target or enough contrast and enough frequencies/shapes/colours to distinguish thousands of heliostats. The achievable accuracies are estimated to be quite high such that fine calibration should be possible.

General disadvantages:

Heliostats far away from the target or those with very small mirror area may not deliver sufficient contrast on the target and are more difficult to measure. Continuous excitation with relevant amplitude leads to effective image broadening.

Advantages and disadvantages related to individual calibration methods:

Beam excitation methods: The use of heliostat drives for excitation, see Bern et al. (2016), does not require any extra installation but limits the frequency space and imposes wear on the drives. It is not yet clear, how many heliostats can be superimposed and separated by their excitation modes in a receiver focal region and how much wear in the drives is caused. In the best case, the procedure works for all heliostats allowing closed-loop tracking control using the sun beam location on the receiver as feedback (M4, see Fig. 2). However, the authors are concerned that it may work only with a reduced number of superpositions of heliostat images limiting the application to open-loop heliostat control with periodic calibration.

Signal beam methods: Using a secondary low-energetic light beam as signalisation (Gross, 2016; Flesch et al., 2012) requires the installation and measurement of the device offset to the heliostat normal prior to using the system which may imply the need for an independent pre-calibration system during the heliostat field commissioning phase. This is because the feedback signal for control is not generated on the target, but with a small device on the heliostat (M3d, see Fig. 2). A general disadvantage of (Flesch et al., 2012) is that the target area will need to be very large if most of the heliostats in a large heliostat field are to be calibrated for most of the day. The same should apply also for (Gross, 2016). If the secondary light beam is generated from sunlight, then the intensity may be too low for heliostats at far distance from the tower and some blurring of the image may occur. The further the distance of a heliostat from the tower, the larger must be the auxiliary mirror in order for a camera on the ground to be able to detect the image on the calibration target. If lasers are used, eye hazard, contrast, and costs may be issues. Finally, the space for the signal beams on a target is limited and the target size will need to be adjusted to fit the movement of the secondary light beam device which differs from the sun trajectory. If the sun is used for obtaining signal beams, the elevation and azimuth angles which can be calibrated depend on the point of time in the year. As an initial effort, a coarse pre-calibration of the heliostats signal beam to focus on the measurement target or receiver is necessary for all described types in class A1b.

4.1.2. Subclass A2: Camera(s) on tower or UAV(s)

Class A2a: Single or multiple photos (photogrammetry)

General advantages:

The techniques of capturing a photo of a heliostat are not widely used yet. However, the advantages of these techniques are that they do not require reflected sunlight and thus they are therefore independent of the point in time in the year and Lambertian target. Moreover, an approximate knowledge of the rough heliostat orientation is not required.

General disadvantages:

Extreme heliostat angles with respect to the camera orientation are more difficult to measure. Heliostats with small elevation angle and reflection of the ground are more complex to detect and process. The distance to heliostats might play a role if the camera's zoom (or lens' focal length) is insufficient or because of atmospheric attenuation or due to flickering that limits the image quality.

Advantages and disadvantages related to individual calibration methods:

Methods with camera on tower or mast: The methods of Röger et al. (2010) and Prahl et al. (2009) require only a simple camera installation at elevated height on the tower (or mast) and can be used for pre-calibration but not for fine calibration. No extra devices are needed. Hines and Johnson (2014) additionally requires the installation of diffracting patterns on each heliostat which enables the method to achieve fine calibration accuracy and might allow closed-loop tracking control, if enough real time image data is available for the total heliostat field. A reference calibration to determine the spatial orientation of the diffracting pattern with respect to the heliostat normal may be required. The concepts with a camera on a tower or mast (Röger et al. 2010; Hines and Johnson, 2014) can be used during plant operation and give almost instantaneous information from just a single image. The concept

described in Prahl et al. (2009) needs images of various heliostat orientations which either can be taken throughout a day during normal operation or by faster movement of the heliostat.

Method with UAV: The airborne camera concept (Jessen et al., 2020) is simple in the sense that no additional installation is necessary, but a UAV as well as flight permissions are needed. The accuracy is that of a coarse calibration. This system might be suitable for pre-calibration, also for tower plants under construction. While the concepts with a camera on a tower or mast (Röger et al., 2010; Hines and Johnson, 2014) can be used during plant operation (heliostat tracking) and give almost instantaneous information from just a single image, the heliostat tracking must be stopped during the whole process of airborne image acquisition of the heliostat field for a correct photogrammetric evaluation (Jessen et al., 2020).

Regarding the central camera-based heliostat field calibration method using stereo photogrammetry investigated by Sauerborn et al. (2013), the accuracy of the calibration method will increase with increasing camera resolutions. The cameras require a tracking system as only one heliostat is measured at a time. Alternatively, several cameras can be installed in the field with a fixed view onto multiple heliostats for a faster measurement of the entire heliostat field.

As the concepts in class A2a do not generate the feedback signal using the sun beam reflected on target, but rely on geometric information of the concentrator (M3c/d, see Fig. 2), the way the heliostat normal is derived by the measurement signals and translates to an aimpoint on the receiver has to be checked carefully. For example, in Röger et al. (2010), Prahl et al. (2009) and Jessen et al. (2020), facets that are not detected would influence the calibration accuracy if the overall heliostat surface normal was determined by a simple averaging of the detected normal vectors.

Class A2b: Reflected image of object (e.g. star, LED, sun/sun's brightness) in a heliostat

Advantages and disadvantages related to individual calibration methods:

The measurable heliostat orientations are only limited by the geometric constellation between the camera and the reflected object. Reflected light from soil on the mirror surface can increase complexity of the detection of the object. The number of normal vectors that can be obtained from a heliostat depends on how many different images are processed with the reflected object in the heliostat. Using a UAV (Prahl et al., 2015), the number of normal vectors that can be obtained depends on the flight route, the pre-orientation e.g. from a prior coarse calibration step and the frequency of image acquisition. Using a star (Arqueros et al., 2003; Hines, 2016), it depends on measurement time and earth rotation. While having a moving camera or a moving object, different heliostat orientations can be characterised sequentially. Using the tower edge as reflected image (Mitchell and Zhu, 2019), the camera can be actively moved to obtain a wider characterisation of the azimuth movement of the heliostat. Regarding the method described by Schell (2011), the advantage is that dozens of heliostats can be calibrated simultaneously. The disadvantages are that the heliostats must be driven out of focus which leads to less power being available on the receiver and that the calibration process for an entire heliostat field with thousands of heliostats may consume a lot of time.

Regarding the measurement with an airborne camera (i.e. UAV), no additional infrastructure is necessary. Therefore, this calibration method is especially suitable for first calibrations during a heliostat field commissioning phase and fast plant ramp-ups. For the other reflection methods, a tower (or mast) has to be available to mount the camera (Arqueros et al., 2003; Hines, 2016) or the LEDs (Zavodnya et al., 2015).

The feedback signal for control is generated on several points on the mirror surface (M3c, see Fig. 2). Hence, while calculating the heliostat normal, special attention has to be drawn on how the sampled mirror surface data of the heliostat are processed to generate the heliostat normal. A closed-loop tracking control operation for the whole heliostat field is not possible while using a UAV, or a star.

It is generally possible to identify images reflected over long distances. However, local slope deviation errors cause significant distortions at long distances. For this reason, a moving airborne camera may have advantages to optimise the distances between heliostat and camera, especially for large solar fields.

4.1.3. Class B: Central laser or radar based measurement methods

(i) Central laser and cameras

Advantages:

The method using a central laser and cameras is currently in the proof-of-concept stage. The concept foresees that the method works with all heliostat types of any shape and size and it allows the orientation measurement of individual facets. Modifications to the heliostat or special communication technology are not necessary. A heliostat does not require a highly accurate and precise drive mechanism as long as the measurement interval per heliostat is small (for instance, every few minutes). With the use of e.g. 3-D rotary stage piezo motors, the laser beam can be directed towards individual heliostat facets at a high accuracy and precision. High laser scanning rates can be achieved. In normal operation of the central laser method, a Lambertian screen is not necessary. However, for purposes of pre-calibrating the central laser and camera system, a Lambertian screen might still be used. The central laser and camera method has the potential to be relatively cheap as the only investment is the laser, the dual-axes laser tracker as well as two or more cameras with spectral filters in or around the heliostat field. A major advantage of this calibration method is that the orientation of individual facets can be measured such that multiple mirror normals can be obtained for each heliostat from which an accurate flux distribution on the receiver can be calculated.

Disadvantages:

Only one facet can be measured at a time. Quick image processing is therefore of essence in order for this method to be competitive. The scattered light intensity of the laser beam is quite low as the energy per pulse must be limited such that it is eye-safe due to reasons of laser safety for protecting staff working in the heliostat field, civilians near the plant as well as pilots and passengers of civilian or military aircraft. Physical effects must be accounted for e.g. the jittering of the laser beam (especially in hot climate due to air density fluctuations), which may lead to high flux hotspots, as well as terrestrial scintillation. Moreover, the central laser method requires special, niche camera and spectral filter technology. The accuracy of the method depends on the camera resolution and quality of image processing. For this method to generally be successful, it is necessary to accomplish high-speed image processing and a very fast and precise laser tracking mechanism. In order to aim the laser beam onto individual facets it may be necessary to use an additional aiming system for the laser. The central laser and cameras method covers the signal path M1 to M3c/M3d and is not fast enough to be used for closed-loop tracking control.

(ii) Central total station

Advantages:

The main advantage of the concept to calibrate the heliostats with a total station is the independence from the sun. Due to this fact, the

calibration process can be done at the time when it does not influence the electricity production. In addition to that, also the installation of the total station on top of the power tower is relatively simple. Depending on the type of solar field and field of view, it is possible that only one total station is required. Regarding the accuracy, a fine calibration of the heliostats is generally achievable, especially for bigger heliostats.

Disadvantages:

Although using a total station for calibration has several advantages, the disadvantages are predominating. There are high investment costs for the measurement system with one total station (EUR 50 k) plus approximately EUR 30 per heliostat for three prims. Labour costs are not included in the named costs. The effort for the installation of the prisms onto the heliostats depends on the heliostat model and can be very time-consuming, especially because the alignment of the prisms is very important. The prism plane must be identical to that of the mirror plane (same normal vectors) or else a pre-calibration process of each heliostat has to be carried out. Besides that, it is mandatory for the total station to allocate the prims to the corresponding heliostat, which can be difficult to achieve in practice, especially with small distances between the prisms of two heliostats. In addition to that, the total station is only capable of saving and measuring a limited number of prisms per scan, which means that the measurement field needs to be adjusted very often. Another disadvantage is the necessary coarse orientation of the heliostats towards the total station because of the limited entrance angle of the prisms. The central total station method covers the signal path M1 to M3c/M3d and is not fast enough to be used for closed-loop tracking control.

(iii) Central radar
Advantages:

The calibration process can take place not only during plant operation but also during cloudy conditions and during the absence of solar irradiance. Moreover, the method can be used for other applications such as determining the shape of the mirror surfaces. Large groups of heliostats can be measured simultaneously.

Disadvantages:

It is necessary to install three corner reflectors per heliostat which increases the effort during the heliostat construction phase. The reflectors cause additional shading and blocking which cannot be avoided. It is not possible to scan the entire heliostat field at once, rather it is only possible to scan groups of heliostats. The central laser method covers the signal path M1 to M3c/M3d and is, in the current development stage, not fast enough to be used for closed-loop tracking control.

(iv) Central laser scanner
Advantages:

Same as for central radar.

Disadvantages:

The described measurement method by means of scanning the backside of heliostats is not practical. For frontal measurement of heliostats, it is necessary to install reflectors on the mirror surfaces. The laser scanner method covers the signal path M1 to M3d and is, in the current development stage, not fast enough to be used for closed-loop tracking control.

4.1.4. Class C: Central solar focus position detection with cameras or sensors on tower

The methods (i) to (iv) cover the signal path M1 to M4 and are fast enough to be used as online calibration system (closed-loop tracking control).

(i) Several Cameras or Sensors around Receiver
Advantages:

The required hardware around the receiver, i.e. cameras for the methods described by Kribus et al. (2004) and Coquand et al. (2017) is standard off-the-shelf and relatively easy to install. No additional hardware in the heliostat field is required. The cameras can view the entire heliostat field such that a simultaneous calibration of all the heliostats is possible. The methods with sensors around the receiver from Convery (2011) and Freeman et al. (2015), sensors are also standard off-the-shelf and relatively easy to install.

Disadvantages:

A coarse calibration is necessary with an extra effort of directing the heliostats to the receiver. The software to determine the aiming errors, identify the single heliostats and give the correction pairs to the process control system is relatively complex and must be developed individually. The methods described by Convery (2011) and Freeman et al. (2015) use sensors around the receiver, so in order to be able to distinguish between individual heliostats a signalisation is required. Both methods foresee the installation of piezo-electric actuators for imposing a vibration on each heliostat's mirror surface to create a signalisation via beam excitation, which leads to an additional investment in the solar field. The access to the cameras for maintenance (e.g. cleaning) may be difficult. Depending on the distance of the cameras from the receiver, the cameras may need to be able to withstand moderate to high flux irradiance. This could require complex cooling and expensive camera systems.

(ii) Several Cameras embedded in Receiver:
Advantages:

The installation of camera obscuras embedded in the receiver should not pose any technical issues. Highly detailed flux maps on the receiver are obtained.

Disadvantages:

Availability of space for placing the cameras in the receiver structure, accessibility of camera if placed behind receiver tubes, large camera design necessary to avoid diffraction of light. The camera system must be able to withstand high flux irradiance. This could require complex cooling and expensive camera systems.

(iii) Camera Array on Moving Bar moved along Receiver:
Advantages:

In the method of Collins et al. (2017), the cameras in the moving bar can view the heliostat field within their field of view such that a calibration of these heliostats is possible after a sweep across the receiver surface is completed.

Disadvantages:

The access to the cameras for maintenance (e.g. cleaning) may be difficult. When the bar moves along the receiver surface it blocks a

small portion of the concentrated irradiance. The cameras must be able to withstand high flux irradiance while in the solar focus. This could require complex cooling and expensive camera systems. During the sweep, wind gusts could cause heliostats to move, which may be unfavourable for the measurement.

(iv) Camera Array or Sensor Array as Target

Advantages:

The methods from Gross (2016) have the potential of being very fast and very accurate, allowing indirect closed-loop tracking control when using an array of digital cameras, optical sensors or photodetectors as target on the tower.

Disadvantages:

The main disadvantages from the methods from Gross (2016) are that small auxiliary mirrors must be installed onto each heliostat and that a camera or sensor array must be fitted as the target which adds complexity. If sensors are used, then the auxiliary mirrors need signal encoding. It should also be noted that the auxiliary mirror method only gives feedback regarding the theoretical heliostat's normal but not on the orientation of individual facets. The access to the cameras for maintenance (e.g. cleaning) may be difficult.

4.1.5. Class D: Cameras or sensors on each heliostat

Cameras or sensors on each heliostat

Advantages:

Mounting of cameras or non-optical sensors can be easily accomplished, and the necessary technology is available as mass products at low prices. In most cases, the cameras or sensors can be attached anywhere on the heliostat and merely require pre-calibration in the field before going into operation. Depending on the calibration method, either one or multiple detectable objects must be visible to the camera during calibration or tracking control. Detectable objects can be the sun, receiver, tower, retroreflectors, passive targets or active targets such as visible or infrared lights. The image processing is fast enough to enable quasi-realtime orientation detection locally on each heliostat. These methods usually cover the signal path M1 to M3b and are fast enough to be used for closed-loop tracking control. As an exception, the method described by Fairman et al. (2019) can be named which covers the signal path M1 to M4. Each method measures the orientation individually for each heliostat. The accuracy, precision and the time to determine the orientation depend mainly on the used hardware. Modern commodity hardware such as camera chips as used in mobile phones, single board computers such as Raspberry Pi or Arduino can be used for achieving high accuracy, but its deployment in and shielding from harsh, hot weather conditions should be tested thoroughly. Hickerson and Reznik (2008) describe a method of shielding the camera by means of mounting the camera at the back of a reflector in forward facing direction and allowing the camera to look through a small area of the reflector where the reflective coating has been removed. Similarly, Burisch et al. (2018b) describe the integration of the camera into the reflector during the manufacturing process whereby the camera is protected by the glass layer. As for the latter two shielding methods, by cleaning the reflector during heliostat field maintenance works, the camera will again have a clear view. It is generally possible to retrofit any existing heliostat field with this system. Since the cameras are fixed to the moving reflector, the resulting signal is directly correlated with the heliostat normal.

Disadvantages:

An initial calibration of the camera or sensors is required to determine the orientation and position of the camera or sensors relative to the moving reflector surface normal. A periodic recalibration is recommended to identify whether influences on the hardware occurred (e.g. distortion of heliostat frame, camera position moved). Additionally, another calibration method may need to be applied to compensate for measurement errors in the signal chain (such as lens distortion associated with cameras, etc.). For cameras viewing the sun in combination with other objects, the large difference in object radiation intensity is a challenge for image recognition.

Depending on the camera position and orientation, dust settlement may also have an impact on the accuracy of image recognition. Regular lens cleaning might be required if the camera is not shielded. It is not possible to measure the orientation of individual facets unless each facet is equipped with its own camera. The specific cost of the calibration system increases with the decrease in heliostat size. The accuracy depends on the camera resolution and effectiveness of the image processing code. Methods with non-optical sensors are practical only if in the future the problems with drift and accuracy can be solved. Especially sensors for measuring the azimuthal direction are not yet accurate enough for an affordable price.

In the case of Sauerborn et al. (2013), although a measurement accuracy of 0.06 mrad can be theoretically achieved with calibrated magnetic encoded sensors, it is very difficult to concentrically align the sensor with the circular magnet. If not aligned sufficiently accurate, as was the case in the experiments, the measurement accuracy drops well below expectations. Moreover, shape changes in the heliostat frame or pylon over time will result in further inaccuracies. This method covers the signal path M1 to M3d.

With the method of Swart (2017), all heliostats can be calibrated simultaneously, but the main disadvantage is the sensitivity to noise as well as other inaccuracies. This method covers the signal path M1 to M3c/M3d.

5. Conclusion

This paper presents a detailed overview on heliostat field calibration methods. In total, about 30 state-of-the-art and new methods have been reviewed and classified in detail. As no standard for definitions of terms exists, relevant general and specific terms were defined. This is a basis which can result in a future guideline in this field of research and application. Such a guideline could be in a similar form to the SolarPACES *Heliostat Performance Testing Guideline* (Röger et al., 2020). In the descriptions of calibration methods, the signal or effect flow from the desired aimpoint set in the control room to the sun beam on the receiver is presented as well as different monitoring or measuring devices (such as encoder, sensor, camera readings etc.) along the signal chain. For ensuring clarification when referring to control and tracking methods (open or closed-loop control), the authors strongly recommend that it should be explicitly stated at which point in the signal chain the feedback signal is generated and which part of the whole chain is covered by the control loop.

Several criteria to classify calibration systems and resulting classes were identified. This publication applied the classification criteria *Location, type and number of measuring devices or sensors.* The classification resulted in four classes A to D and their subclasses. The main classes are *central camera(s) or sensor(s)* (class A), *central laser or radar based measurement methods* (class B), *central solar focus position detection with cameras or sensors on tower* (class C) as well as *cameras or sensors on each heliostat* (class D).

Each calibration system is described in detail which includes, for

instance, information on the achieved accuracy, time per measurement, number of normal vectors created, suitability for fine or coarse calibration, amongst other parameters. A final assessment with the advantages and disadvantages of classes and individual calibration methods concludes the paper. A ranking of calibration methods was explicitly not made because each individual calibration method has its own specific advantages and disadvantages, as listed in detail in the assessment chapter.

Acknowledgements

The project partners and authors would like to express their sincere gratitude to the German federal state of North Rhine-Westphalia for funding the research project HeliBo (FKN PRO 0070 A-E) within the funding programme progres.nrw – Innovation.

References

Arqueros, F., Jimenez, A., Valverde, A., 2003. A novel procedure for the optical characterization of solar concentrators. Sol. Energy 75, 135–142. https://www.sciencedirect.com/science/article/abs/pii/S0038092X03002597?via%3Dihubhttps://doi.org/10.1016/j.solener.2003.07.008.

Belhomme, B., Säck, J.P., Schiricke, B., Schwarzbözl, P., 2011. Device for guiding solar radiation. Patent number: WO002011018367A2.

Berenguel, M., Rubio, F.R., Valverde, A., Lara, P.J., Arahal, M.R., Camacho, E.F., López, M., 2004. An artificial vision-based control system for automatic heliostat positioning offset correction in a central receiver solar power plant. Sol. Energy 76, 563–575. https://www.sciencedirect.com/science/article/abs/pii/S0038092X0300464Xhttps://doi.org/10.1016/j.solener.2003.12.006.

Bern, G., Schöttl, P., Heimsath, A., Nitz, P., 2016. Novel imaging closed loop control strategy for heliostats. In: SolarPACES 2016.

Bezares del Cueto, J.L., Safar Sideq, M., Núñez Clemente, D., Bezares del Cueto, J., 2017. Method and system for calibration of a plant of heliostat in a thermal solar concentration plant. Patent number: ES2595637B1.

Burisch, M., Olano, X., Sánchez, M., Olarra, A., Villasante, C., Olasolo, D., Monterreal, R., Enrique, R., Fernández, J., 2018a. Scalable HeliOstat calibRation sysTem (SHORT) – calibrate a whole heliostat field in a single night. In: AIP Conference Proceedings 2033, 040009 (2018). https://doi.org/10.1063/1.5067045.

Burisch, M., Sánchez, M., Villasante Corredoira, C., Aranzabe Basterrechea, E., 2018b. Mirror for a solar reflector, method of mirror assembly and management system in a solar field. Patent number: WO/2018/069558.

Carballo, J.A., Bonilla, J., Berenguel, M., Fernández-Reche, J., García, G., 2019. New approach for solar tracking systems based on computer vision, low cost hardware and deep learning. Renewable Energy 133, 1158–1166. https://doi.org/10.1016/j.renene.2018.08.101.

Collins, M., Potter, D., Burton, A., 2017. Design and simulation of a sensor for heliostat field closed loop control. In: AIP Conference Proceedings 1850, 030009 (2017). https://doi.org/10.1063/1.4984352.

Convery, M.R., 2011. Closed-loop control for power tower heliostats. In: SolarPACES 2011.

Convery, M.R., 2013. System and method for aligning helostats of a solar power tower. Patent number: US 8,344,305 B2.

Dabrowksi, J., Göttsche, J., Dr., Nettelroth,V., Sauerborn, M. Dr., 2014. Method for position- and orientation determination of heliostat having mirror face, involves irradiating mirror face of heliostat with laser beam having predetermined wavelength. Patent number: DE 10 2013 207 022 B3.

Díaz-Félix, L.A., Escobar-Toledob, M., Waissmanc, J., Pitalúa-Díaza, N., Arancibia-Bulnesd, C.A., 2013. Evaluation of heliostat field global tracking error distributions by Monte Carlo simulations. In: SolarPACES 2013, Energy Procedia 49 (2014) 1308–1317. https://doi.org/10.1016/j.egypro.2014.03.140. https://www.sciencedirect.com/science/article/pii/S1876610214005943.

Coquand, M., Caliot, C., Hénault, F., 2017. Backward-gazing Method for Heliostats Shape Measurement and Calibration. In: AIP Conference Proceedings 1850, 030010 (2017). https://doi.org/10.1063/1.4984353.

Duffie, J.A., Beckmann, W.A., 2006. Solar Engineering of Thermal Processes, third ed. Wiley, New Jersey.

Fairman, P., Farrant, D., Connor, P., 2019. Closed loop optical tracking of heliostats. AIP Conference Proceedings 2126, 030021 (2019). https://doi.org/10.1063/1.5117533.

Flesch, R., Belhomme, B., Ahlbrink, N. and Pitz-Paal, R., 2012. Automatic Determination of Heliostat Orientation Using an Auxiliary Mirror. In: SolarPACES 2012.

Freeman, J., Keerthi, K.S., Chandran, L.R., 2015. Closed loop control system for a heliostat field. In: International Conference on Technological Advancements in Power and Energy (TAP Energy), Kollam, 2015, pp. 272–277. https://doi.org/10.1109/TAPENERGY.2015.7229630.

Freeman, J.D., et al., 2014. Study of the errors influencing heliostats for calibration and control system design. In: IEEE International Conference on Recent Advances and Innovations in Engineering (ICRAIE-2014), May 09-11, 2014, Jaipur, India. https://doi.org/10.1109/ICRAIE.2014.6909113.

Goldberg, N., Kroyzer, G., Hayut, R., Schwarzbach, J., Eitan, A., Pekarsky, S., 2015. Embedding a visual range camera in a solar receiver. Energy Procedia 69, 1877–1884. https://linkinghub.elsevier.com/retrieve/pii/S1876610215004750https://doi.org/10.1016/j.egypro.2015.03.169.

Gross, W., 2016. Closed loop tracking system using signal beam. Patent number: US 9,523,759 B2.

Gross, F., Balz, M., 2019. Potentially confusing coordinate systems for solar tower plants. In: SolarPACES 2019, Daegu, South Korea.

Harper, P.J., Dreijer, J., Malan, K., Larmuth, J. and Gauche, P., 2016. Use of MEMs and optical sensors for closed loop heliostat control. AIP Conference Proceedings 1734, 070015; https://doi.org/10.1063/1.4949162.

Hickerson, K., Reznik, D., 2008. Heliostat with integrated image-based tracking controller. Patent number: WO/2008/121335.

Hickerson, K., Reznik, D., 2012. Heliostat with integrated image-based tracking controller. Patent number: US 8,153,945 B2.

Hines, B.E., Johnson, R.L., 2014. Apparatus and method for pointing light sources. Patent number: US20140110560 A1.

Hines, 2016. Heliostat characterization using starlight. Patent number: WO2016205612A1.

Jessen, W., Prahl, C., Röger, M. Pitz-Paal, R., 2020. Airborne photogrammetric heliostat pre-calibration, DLR, to be published in 2020.

Jones, S.A., Stone, K.W., 1999a. Analysis of solar two heliostat tracking error sources. In: 1999 ASME International Solar Energy Conference; Maui, HI; 04/11-14/1999.

Jones, S.A., Stone, K.W., 1999b. Analysis of strategies to improve heliostat tracking at Solar Two. Sandia National Laboratories, SAND99-0092C.

King, D.L., Arvizu, D.E., 1981. Heliostat characterization at the central receiver test facility. J. Sol. Energy Eng. 103, 82–88. https://doi.org/10.1115/1.3266229.

Koningstein, R., 2012. Optical signal aiming for heliostats. Patent number: US 2012/0279485 A1.

Koningstein, R., Fitch, J. S., Ricket, D. J., Mo, V., 2012. Heliostat control scheme using cameras. Patent number: US 2012/0174909 A.

Kribus, A., Vishnevetsky, I., Yogev, A., Rubinov, T., 2004. Closed loop control of heliostats. Energy 29 (5–6), 905–913. https://www.sciencedirect.com/science/article/abs/pii/S0360544203001956https://doi.org/10.1016/S0360-5442(03)00195-6.

Malan, K.J., 2014. A Heliostat Field Control System. Master's thesis, Stellenbosch University. http://scholar.sun.ac.za/bitstream/handle/10019.1/86674/malan_heliostat_2014.pdf?sequence=1 (last accessed 17 January 2020).

Mancini, T., 1999. Heliostat daily centroid shift. IEA SolarPACES report no. III-1/99.

Mitchell, R., Zhu, G., 2019. A sensitivity study on a non-intrusive optical (NIO) method to measure optical errors of heliostats in utility-scale power tower plants. In: SolarPACES 2019, Deagu, South Korea.

Pfahl, A., Buck, R., Rehschuh, K. 2009. Method for controlling the alignment of a helostat with respect to a receiver, heliostat device and solar power plant. Patent No.: US 8,651,100 B2.

Pfahl, A., Rheinländer, J., Krause, A., Buck, R., Giuliano, S., Hertel, J., Blume, K., Schlichting, T., Janotte, N., Ries, A., 2019. First lay-down heliostat with monolithic mirror-panel, closed loop control, and cleaning system. In: AIP Conference Proceedings 2126, 030042 (2019). https://doi.org/10.1063/1.5117554.

Prahl, C., Göhring, F., Röger, M., Hilgert, C., Ulmer, S., 2015. Verfahren zur Vermessung von Heliostaten. Patent DE 10 2015 217 086 B4. Procedimiento para la medición de heliostatos, Patent number: ES000002604554B2.

Prahl, C, Röger, M., Kiewitt, W., 2009. Advances in optical measurement techniques for solar concentrators. In: SolarPACES 2009, September 15-18, Berlin, Germany, 2009, ISBN 978-3-00-028755-8.

Röger, M., Prahl, C., Jessen, W., Schwarzbözl, P., Sattler, J., Niederwestberg, S., Göttsche, J., 2018. Verfahren zur Vermessung und Kalibrierung von Heliostaten. 21. Kölner Sonnenkolloquium. https://elib.dlr.de/122783/.

Röger, M., Prahl, C., Ulmer, S., 2010. Heliostat shape and orientation by edge detection. J. Sol. Energy Eng. 132 (2), 21002. https://doi.org/10.1115/1.4001400.

Röger, M., et al., 2020. Guideline for heliostat performance testing. In: SolarPACES Task III Guideline. http://www.solarpaces.org/tasks/ (publication planned in Solar Energy 2020).

Sánchez González, M., Olarra Urberuaga, A., Villasante Corredoira, C., Olasolo Don, D., Burisch, M., 2017. Calibration method for heliostats. Patent: WO2017055663A1.

Sánchez, M., 2018. Scalable HeliOstat calibRation sysTem (SHORT) – How to calibrate your whole heliostat field in a single night. Protermosolar 09/02/2018. http://www.solarconcentra.org/wp-content/uploads/2018/02/Scalable-HeliOstat-calibRation-sysTem.-CENER.pdf (last accessed 3 February 2020).

Sauerborn, M., Göttsche, J., Hoffschmidt, B., 2013. Machbarkeitsstudie zur Entwicklung einer radargestützten Positionsregelung von Heliostatenfeldern für Solarturmkraftwerke (HelioScan). Schlussbericht, TIB Hannover.

Sauerborn, M., Klimek, J., Hoffschmidt, B., Sieger, S., Biegel, G., Essen, H., Göttsche, J., Hilger, P. 2012. Determination of heliostat mirror orientation by radar technology. In: SolarPACES 2012, Marrakesh, September 11–14.

Schell, S., 2011. Design and evaluation of esolar's heliostat fields. Sol. Energy 85 (2011), 614–619. https://doi.org/10.1016/j.solener.2010.01.008.

Stone, K.W., 1986. Automatic heliostat track alignment method. Patent number 4,564,275 issued 1986.

Swart, B.D., 2017. A method for accurate measurement of heliostat mirror orientation. Master's thesis, Stellenbosch University. sterg.sun.ac.za/wp-content/uploads/2010/

11/71.pdf (last accessed 3 February 2020).
NREL, 2020. National Renewable Energy Laboratory. https://solarpaces.nrel.gov/by-technology/power-tower (last accessed 17 January 2020).
van den Donker, P., Rosinga, G., du Marchie van Voorthuysen, E., 2016. Reducing heliostat field costs by direct measurement and control of the mirror orientation. AIP Conference Proceedings 1734, 020025. https://doi.org/10.1063/1.4949049.
Yogev, A., Krupkin, V. 1999. Control of a heliostat field in a solar energy plant. US Patent Number: 5,862,799. Patent issue date: 26 January 1999.
Zavodnya, M., Slack, M., Huibregtse, R., Sonn, A., 2015. Tower-based CSP artificial light calibration system. Energy Procedia 69, 1488–1497. https://doi.org/10.1016/j.egypro.2015.03.098.